SeanPaul La Selle

Deposits of the 1969 Ozernoi and 1971 Kamchatsky tsunamis at the heads of submarine canyons

Department of Earth and Space Science, University of Washington

In partial fulfillment of a non-thesis Master's degree

12 December, 2012

ABSTRACT: The inundated local areas of both the 1969 Ozernoi and 1971 Kamchatsky tsunamis in Kamchatka, Russia included shorelines adjacent to the heads of large submarine canyons. The preserved sandy deposits of these tsunamis have been mapped in previous studies along the northern and eastern coasts of the Kamchatsky Peninsula, but not along the southern shoreline near the town of Ust Kamchatsk, located at the head of one of the largest submarine canyons in Kamchatka. Near Ust Kamchatsk, we interpret the sandy deposit above the historical 1964 ash layer to be a tsunami deposit based on the inland distances (~200 m) and elevations (~6 m) achieved by the deposit. Models of tsunami inundation for the 1969 and 1971 events account for most of the observed sediment runup along the Kamchatsky and Ozernoi Peninsulas, but the models do not reach the sediment runup at Ust Kamchatsk and Stolbovaya, another locality with a submarine canyon just offshore. Detailed tsunami modeling indicates that the submarine canyons refracted tsunami waves toward the canyon walls, decreasing offshore wave height at the head of the canyon. However, this pattern is not reflected in modeled or sediment runup. The high local peak in sediment runup observed at Ust Kamchatsk, along with the low modeled runup suggests that a local submarine landslide-generated tsunami is responsible for the high sediment runup. The pattern of sediment runup in Stolbovaya is not as indicative of a submarine landslide source, but there is still a discrepancy between modeled and sediment runup.

INTRODUCTION AND BACKGROUND

The sedimentary deposits of tsunamis are commonly the primary source of data used to inform reconstructions of prehistoric and unobserved tsunamis and events in sparsely populated regions. Tsunami modeling can add more detail to these reconstructions when corroborated with the measured distribution of tsunami deposits. A multitude of factors can influence tsunami inundation, ranging from complex earthquake slip distributions to small variations in onshore local topography. As a result, modeled inundation and inundation marked by tsunami deposits sometimes conflict with each other, which requires revisiting the sedimentological interpretation and reevaluating whether or not the model is capturing the most significant physical factors. If the model results and deposit interpretation still stand on their own, other tsunami sources and processes may explain the discrepancy, adding important elements to the reconstruction of a given tsunami.

Kamchatka (Figure 1) is an excellent region to study tsunamis and tsunami deposits, primarily because of the frequent occurrence of nearby tsunamigenic earthquakes and the abundance of tephra layers that provide age control. In most localities, tsunami recurrence intervals over at least the last 3000 years can be determined (*Pinegina and Bourgeois, 2001)*. Within the past century there have been at least 7 significant, locally produced tsunamis (Figure 1). However, not all of these earthquakes and tsunamis were well observed due to the sparse population and a lack of instrumentation on the Kamchatka Peninsula. As a result, reconstructing these recent tsunamis requires extensive field observations of the preserved tsunami deposit in addition to running computer models of the tsunami in order to fill in details not recorded by the deposit (*MacInnes et al., 2010*). Two of these recent events, the 1969 Ozernoi and 1971 Kamchatsky tsunamis, went largely unobserved on the Kamchatsky Peninsula (Figure 2) despite inundating much of the shoreline. Later field work (*Bourgeois and Pinegina, 2001 and Martin et al., 2007*) identified deposits of both tsunamis between Kamchatsky Cape and north of the Ozernoi Peninsula. *Martin et al. (2007)* also modeled the 1969 and 1971 tsunamis and demonstrated that the earthquake sources were primarily responsible for the distribution of observed tsunami deposit runup (the elevation of the deposit at its furthest inland point). However, both the 1969 and 1971 models produced results that undershot the observed deposit runup at Stolbovaya, a locality at the head of a submarine canyon (Figure 2), despite matching or exceeding deposit runup everywhere else. To explain the discrepancy between the low modeled runup and high deposit runup in Stolbovaya, a submarine landslide was hypothesized as a way to have locally enhanced wave height.

Similar observations and modeled results have been reported for other tsunami events, most notably the deadly 1998 Papua New Guinea tsunami (*Kawata et al., 1999, Gelfenbaum and Jaffe, 2003*). Using more detailed bathymetry (200 m resolution offshore, and 22 m resolution at depths less than 200 m) clearly showing the presence of a nearby submarine canyon, an early study came close to matching modeled runup to the observed runup, and described the wave focusing effects of ridges on either side of the canyon and the narrow shelf at its head (*Matsuyama et al., 1999*). However, even more detailed post-tsunami reconnaissance of the local bathymetry identified a large submarine landslide scarp (*Tappin et al., 1999*). By modeling the submarine landslide of a volume suggested by the size of the scarp, researchers suggested that the locally high runup in Sissano Lagoon was attributable to a landslide-generated tsunami (*Lynett et al., 2003*) rather than the smaller, earthquake-generated wave. Despite being one of the most thoroughly studied recent tsunamis, the proposed submarine-landslide source is still controversial.

Without access to very high-resolution bathymetry in Kamchatka, we cannot conclusively determine if a submarine landslide was responsible for the locally high runup at Stolbovaya. Nevertheless, we can use the characteristics of the 1969 and 1971 tsunami deposits along with detailed tsunami inundation modeling to rule out the earthquake sources and identify if there is still a need to invoke a submarine landslide. In this paper I investigate the nature of the 1969 and 1971 tsunami deposits near the heads of three submarine canyons and characterize the bathymetric effects of these canyons on tsunami runup by modeling tsunami propagation and inundation. I also extend the observations of the 1971 tsunami deposit to include the Ust Kamchatsk region (Figure 2).

Setting and Field Localities

Bathymetry

Study areas were selected based on their proximity to submarine canyons in order to determine if there is any regularity to the sedimentological characteristics and distribution of tsunami deposits. Most of the detailed sedimentological data presented in this paper was collected in 2010 and 2011 near Ust Kamchatsk. I targeted this locality due to the presence of Kamchatsky Canyon, which dictates the variable character of offshore bathymetry in northern Kamchatsky Bay (Figure 2). Kamchatsky Canyon is one of the largest submarine canyons along the Kamchatka Peninsula (Gnibidenko et al., 1984) and extends over 175 km from offshore the mouth of the Kamchatka River to the deepsea trench, at 4500 m depth. Within the confines of northern Kamchatsky Bay, the canyon has several branching arms, which merge into a single large channel around 2.5 km wide in deeper water. One of main, branching channels is directed towards the east end of Dembi Spit. To the west of Ust Kamchatsk, the continental shelf is 8-15 km wide, and narrows eastward to Ust-Kamchatsk where the canyon cuts into the shelf. The shelf is only 1 km wide along the eastern side of the canyon, whose edge drops down to a kilometer depth within 7 km offshore between the Mutnaya River and Kamchatsky Cape. Off shore of Kamchatsky Cape is a broad ridge that sits between Kamchatsky Canyon and a smaller, unnamed canyon to the east. The head of this smaller canyon is directed towards the mouth of the Perevalnaya River.

The major bathymetric feature in southern Ozernoi Bay is Pokatiy Canyon. Unlike Kamchatsky Canyon, Pokatiy Canyon has just one very well-defined channel, extending 75 km offshore. In the vicinity of the study area, the shelf width varies from 1 km (along the head of the canyon) to 5 km at the mouth of the Stolbovaya River.

Ust Kamchatsk

Ust Kamchatsk is a small town situated next to mouth of the Kamchatka River at the northern end of Kamchatsky Bay (Figure 3). To the north of Ust Kamchatsk is Nerpich'e Lake, a large brackish lake which is bounded to the south by Dembi Spit. The lake is open to the Pacific Ocean through the river mouth. Dembi Spit extends 8 km westward from the southeast corner of Kamchatksy Peninsula, ending at the left bank of the Kamchatka River. Part of the town of Ust Kamchatsk is located along the western half of the spit. Based on the oldest preserved tephra found on the spit ($Shiveluch_{1450}$) Dembi Spit emerged at least 1300 calendar years ago, now rising more than 10 m above sea level in some places. The region west of Ust Kamchatsk on the right bank of the river is an accretionary coastal plain ("Gorbusha"), characterized by relatively low ridges and swales.

Stolbovaya

The Stolbovaya locality is at the southern end of Ozernoi Bay in the Bering Sea, 55 km north of Ust Kamchatsk (Figures 2,3). This region is also an accretionary coastal plain (*Bourgeois et al.*, *2006*), with peat present locally. The mouth of the Stolbovaya River is located at the east end of the embayment, with rocky headlands farther east.

The 1969 and 1971 earthquakes and tsunamis

1969

On 23 November, 1969 at 11:10 local time, a M_w 7.7 reverse thrust earthquake occurred in Ozernoi Bay (*Gusev and Shumilina, 2004*). The resulting tsunami was directed towards the southern portion of the Ozernoi Peninsula. Tsunami runup was observed at a few locations along the coastline and generally reported to be 5-7 meters. At the mouth of the Ol'khovaya River (along the central portion of Ozernoi Bay) witnesses reported 10-15 meters of runup, but this observation was likely exaggerated, based on the lower runup measured in subsequent field surveys. The tsunami was measured on a tide gauge in Ust Kamchatsk (Figure 4), with a maximum wave height of 20cm. Tide gauges in the Aleutians and Hawaii also observed the tsunami (Table 1)

1971

The 1971 tsunami was the larger of the two events, generated by a M_w 7.8, oblique thrust earthquake (*Cormie,r 1971, Okal &Talandier, 1986*) south of Kamchatsky Cape (Figure 4). The earthquake occurred on 15 December, 1971 at 20:30 local time. The Ust Kamchatsk tide gauge detected the arrival of the tsunami 20 minutes after the earthquake, which also happened to coincide with low tide (-0.5 m). The first wave was the largest, measured at 47 cm at the tide gauge. The earthquake damaged buildings in the area, but there were no reports of tsunami damage, although the wave caused ice to crack up to 1 km upstream from the mouth of the Kamchatka River (*Zayakin and Luchinina, 1987*). The tsunami also registered on tide gauges in the Aleutians and Hawaii with amplitudes twice as large as the 1969 event (Table 1).

TSUNAMI DEPOSITS

Methods

Fieldwork was performed during the summers of 2010 and 2011 in Ust Kamchatsk. Tsunami deposit data for Stolbovaya, the outer Kamchatsky Peninsula, and the Ozernoi Peninsula were collected in 2010 and in previous field seasons by *Bourgeois et al. (2006) and Martin et al. (2007),* using similar methods as described below.

In order to determine the spatial extent of the tsunami deposits in Ust Kamchatsk, we surveyed 9 topographic profiles to distances at least 200 m inland and perpendicular to coastlines (Figure 5). These profiles were spread out over 10 km between Dembi Spit and the Mutnaya River. Surveyed elevations were benchmarked to high tide markers, or the first appearance of permanent vegetation. As in previous studies (e.g. *Martin et al., 2008, Bourgeois et al., 2006, Minoura et a.l, 1996*), we described the stratigraphy of multiple small excavations along each profile (Figure 5). Candidate layers for the 1969 or 1971 tsunami deposits were identified in the field as sandy layers overlying a marker tephra from the 1964 eruption of Shiveluch (SH_{1964}) and traced to their maximum inland extents.

Elevation at tsunami inundation limit is called runup and in this case, we use the inland sediment limit as a proxy for runup. We report sediment runup relative to high high tide markers, or to the first appearance of vegetation. The sediment inundation limit marked by the deposits along Dembi Spit, and on several profiles in Stolbovaya, are located behind high ridges, so overtop heights, the elevation of the highest topography "overtopped" by the deposit, are used to define "runup." The overtop height therefore gives a minimum estimate of tsunami runup, and is limited by topography. For example, if the highest point on a profile is just 2 meters, we can only report sediment runup up to 2 m. If an adjacent profile has an overtop height of 5 meters, the reported sediment runup will look much greater, even though it is likely that tsunami inundating the lower profile had the potential to overtop a 5 m high ridge.

Excavations were dug away from signs of obvious human disturbance, most notably along Dembi Spit where a graded road (constructed in 1961) that runs along the entire spit and large ditches dug at the two westernmost profiles. Further west, on settled portions of the spit, the stratigraphy was too disturbed and access was limited, so runup there could only be inferred based on the fact that there was no tsunami damage.

The SH_{1964} marker tephra is easily identifiable in the field as a 2-5 cm thick, medium-sand layer with sharp contacts, and a "salt and pepper" appearance due to an abundance of feldspars and dark mafic grains (Braitseva et al., 1997, Bourgeois et al., 2006). On nearly all of the profiles, SH_{1964} was found only in excavations greater than 100 m from shore, beyond the influence of most storms and beach processes.

The landward extent of very recent storm deposits was identied by tracking the presence of surface sands over a tephra layer from the October 2010 Shiveluch eruption (SH_{2010}). The recent storm inundation limit was recognized as the abrupt transition on the surface from sand to a clean, 1-2 cm thick tephra deposit.

Tsunami deposit identification criteria

To distinguish tsunami deposits from storm or windblown sands in Ust Kamchatsk, I carefully examined the sedimentological, spatial, and temporal aspects of the candidate sand layers. In general, tsunamis erode sediments from the beach and unvegetated surfaces (Pinegina et al., 2003, Jagodziński et al., 2012), and redeposit them inland, leaving behind sheet-like deposits, which thin and decrease in grainsize landwards. Because of the long-wave nature of tsunamis, their deposits tend to penetrate inland much farther than deposits from storm waves and swash. On the other hand, storm surge can also inundate far inland, but typhoons in Kamchatka are weaker they are in Japan and the narrow shelf offshore of the Kamchatsky Peninsula is not conducive for generating a large storm surge (*Scoffin, 1993; Resio and Westerink, 2008*).

Typical tsunami deposit thicknesses range from 0.5 to 30 cm (Morton et al., 2007). It is commonly reported that storm deposits are commonly greater than 30 cm thick and that they abruptly thin landward, while tsunami deposits thin inland more gradually. Tsunami deposits tend to exhibit grading or massive structure, both of which are evidence of rapid deposition. In well preserved deposits, rip-up clasts and mud laminae indicate temporal changes in sediment transport. In comparison, storm sands tend to exhibit more sedimentary structures associated with longer inundation periods and reworking from storm waves. The recent storm sands in Ust Kamchatsk inundated up to 100m with average runup elevations of 3.5m. We therefore only considered sedimentological characteristics of tsunami deposits found at excavations beyond 100m inland and above 3.5m (or landward of topography exceeding 3.5m). Similar criteria were set for the previous studies of deposits in Stolbovaya and along the outer Kamchatsky Peninsula coast. As a result, the sandy deposits above SH_{1964} at these localities have been interpreted to be tsunami deposits, most likely from the 1969 or 1971 tsunamis. This study focuses on the interpretation of sandy layer above SH_{1964} in Ust Kamchatsk, which was not described in previous study.

The deeper stratigraphy in the Ust-Kamchatsk excavations reflects the transition from a nearshore-beach depositional environment (thick, clean, and coarse sands) to the modern, vegetated surface that is beyond the influence of storm inundation (soil layers and preserved tephra) . Significant storm surge from typhoons, occurs every couple of years in Kamchatka (Kovalev et al., 1991), so if storm waves and storm surge is capable of reaching the excavations above 3.5 meters, we would expect multiple sandy deposits above SH_{1964}, overlying a very thick sequence of storm sands. Instead, we observe numerous sandy beds, interspersed within a background of silty soil below the SH_{1964} tephra. A 1-2 cm thick tephra layer identified as "Shiveluch 1450" (^{14}C yr B.P.) (SH_{1450}) tephra was found in several excavations along with 5-10 distinct sand layers between SH_{1450} and SH_{1964}. If we assume these layers were deposited in separate, single events, the minimum recurrence interval is 125 years, or a recurrence rate of eight per thousand years. The maximum tsunami recurrence rate at Stolbovaya is 7 per thousand years (Bourgeois et al 2006), and 10 per thousand years in Kronotskiy Bay (Pinegina et al, 2003), to the south of Kamchatsky Bay. Since it has only been about 50 years since SH_{1964} was deposited and 50-100 years since a known tsunami inundated the shoreline at Ust Kamchatsk , we only expect to see one sand layer above SH_{1964} at the higher elevations on Dembi Spit

The 1971 tsunami inundated a snow-covered surface, so it is likely that the deposit was disturbed by wind and cryoturbation in the months following deposition. There is also ample evidence of more recent bioturbation from roots and animal burrows. Thus the grainsize trends, variations in thickness, and sedimentary structures that are often used to determine the hydrodynamic conditions at the time of deposition have most likely been altered. As a result, we depend more on the spatial distribution of the deposit, rather than the sedimentary character, to identify the 1971 tsunami deposit in Ust Kamchatsk.

Grain Size Analysis

Profile 200 in Ust Kamchatsk was selected for detailed sampling of the sand layer above SH_{1964} because the deposit here was well preserved and not interrupted by the road. Deposits were vertically subsampled for grain size analysis in 1-2 cm intervals using a lab scoop and 2 cm diameter plastic tubes. After collection, samples were dried and organic matter was removed using forceps. The grain size analysis was done using a Retsch Camsizer, a rapid-analysis device that determines grain diameter by optically measuring the cross-sectional area of each grain. The Camsizer is capable of determining grain size within ±1% for sediment between 3 and 30,000 microns (*Moore et al. 2006*). Grain size characteristics such as median grain size and sorting index were then determined using the Folk and Ward Graphical Method (*Folk 1996, Blott & Pye 2001*).

Deposit origin in Ust Kamchatsk

The sand layer above SH_{1964} in Ust Kamchatsk was traced up to 350m inland, with an average inundation distance around 200 m. Average deposit runup (overtop height) is 6 meters (Figure 6), compared to 3.5 m for recent storm sands. The deposit overtop height could be even greater, since the overtop heights east of Dembi Spit are constrained by slightly lower topography. In addition to large inundation distances and runup elevations reached by the deposit, the fact that there is only one sand layer above SH_{1964} that has reached the excavation localities, is suggestive of an infrequent depositional event. As discussed above, evidence of paleotsunamis below SH_{1964} indicate that tsunamis are the only mechanisms capable of depositing thick sandy deposits on the upper surface of Dembi Spit.

The deposit is up to 33 cm thick and massive in structure, gradually thinning inland on most profiles (Figure 7). The profiles on Dembi Spit, eastward to profile 200 all exhibit thick deposits that thin inland, but the furthest east profiles barely reach 5 cm in thickness. The contact between SH_{1964} and the tsunami deposit is typically sharp, though in some excavations the contact is a thin (<1cm), finer-grained zone of sand mixed with pumice. The upper contact of the sandy deposit is not well defined, and often grades upward into a turfy soil. The deposit is predominantly composed of moderately well sorted, coarse sand (Figure 8). Grain size analysis of recent storm and beach sands indicates that grains size and sorting of these surface deposits are nearly indistinguishable from the inferred 1971 tsunami deposit. This is not unexpected because the beach is the primary sediment source for storm and tsunami deposits in this region. Grain size trends along profile 200 (Figure 9) do not exhibit a clear landward fining trend. In fact, the grain size is medium to coarse sand at the thickest portion of the deposit (JB200), coarsens slightly at the second excavation (Divot 1), and remains as coarse sand throughout the rest of the deposit. Vertical grain size trends exhibit weak coarsening upward sequences at each excavation. Reverse grading does not rule out a tsunami source as several studies have observed reverse grading in sandy deposits of the 2004 Indian Ocean tsunami (*Moore et al. (2006)*; *Choowong et al. (2008); Switzer and Jones (2008))*. Massive or reverse grading indicates that the sandy layer in Ust Kamchatsk could have been rapidly deposited, without enough time for coarsest grains to preferentially settle out first. Another possibility is that the deposit was disturbed by a number of different processes following deposition, which could have erased or altered grain size trends.

Based on the high runup, extensive inundation, gradual inland thinning, and stratigraphic uniqueness of the sandy deposit above SH_{1964}, I interpret this layer to be a tsunami deposit from the 1971 Kamchatsky tsunami.

Tsunami deposit runup patterns

Ust Kamchatsk

The pattern of runup across the spit displays a maximum peak (8.3m) on profile 233, at the midpoint of Dembi Spit (Figure 6). The westernmost profile, profile 240, is also relatively high at 7.4 m.   To the southeast, the sediment runup decreases to 5m. In order to determine possible tsunami runup west of profile 240, we surveyed the height of a cemetery (3.5 m) at the easternmost edge of the town . Because no tsunami damage was reported to the cemetery or other buildings in Ust Kamchatsk, the runup to the west of our profiles is assumed to be less than 3.5m.   Inundation also appears to be highest along the spit, decreasing eastward. The pattern of high runup and inundation along the east end of the spit coincides with the presence of thicker tsunami deposits at those excavations (Figure 7).   Despite lower elevation topography at the southeastern most profiles, inundation distances were shorter and the deposits were significantly less extensive compared to the deposits along Dembi Spit.

Stolbovaya

Deposit runup distribution appears fairly uniform, ranging from 1.9 to 6 meters, and with an average of 3.6 m (Figure 10). The highest runup occurs at the eastern end of the embayment and seems rather high because runup is less than 5m on every other profile. Sediment runup has a smaller, secondary peak at Profile 100, where the head of Pokatiy Canyon is directly offshore (Figure 2). Northwest of Profile 100, runup sharply decreases, while it slowly decreases towards the southwest.

Kamchatsky Cape-Cape Africa and Ozernoi Peninsula

Because of the proximity of the outer coast of Kamchatsky Peninsula to the 1971 earthquake, the highest occurrences of sediment runup were on either side of Cape Africa (Figures 11). Average sediment runup is around 6 .1m, slightly lower than at Ust Kamchatsk. Unlike Ust Kamchatsk and Stolbovaya, the sediment runup near the head of the canyon by the Perevalnaya River is low compared to sediment runup at Cape Africa. This could be due in part to the low topography near the mouth of the Prevalnaya river, but the sediment inundation distance is also surprisingly low.

TSUNAMI MODELING

Modeling Methods

GeoClaw

The GeoClaw model was used to simulate the generation, propagation, and inundation of the 1969 and 1971 tsunamis. After undergoing extensive benchmarking (*Gonzalez et al., 2011*), GeoClaw was recently approved by the US National Tsunami Hazard Mitigation Program

(NTHMP) for natural hazards modeling. The first step in modeling is to determine the initial seafloor deformation (and therefore the initial sea-surface disturbance). This is done using the Okada Model, which assumes a finite rectangular fault (*Okada, 1985*), and takes inputs of fault strike, dip, rake, slip, and size. The resulting sea-surface deformation provides the initial conditions for propagating the tsunami over the input bathymetry by solving the nonlinear two-dimensional shallow-water equations with finite-volume methods (*LeVeque, 2002*). Adaptive mesh refinement (AMR), which refines grids around the propagating wave, was used to reduce computational time. In the vicinity of coastlines where runup and inundation were measured in the field, grid refinement factors up to *450* times the starting grid resolution of 0.25 degrees were used and maximum inundation in modeled runs was calculated on fixed grids. Inundation was handled by setting water depth on dry cells to zero, and a positive depth value when wet. Plots of tsunami wave height were generated using the python plotting tools included with GeoClaw. To better visualize inundation patterns, the fixed grid inundation data were exported to ArcGIS and overlain on the DEMs used for modeling and a georeferenced aerial photo of the Kamchatsky Peninsula.

Bathymetry

An integrated bathymetric and topographic DEM was created by stitching a 3 arcsecond DEM of land topography to a 20 arcsecond DEM of offshore bathymetry, which are the highest-resolution DEM products available of this area. In order to match the datasets along the shoreline, bathymetry 500-1000 meters offshore (1-2 cell widths) on the coarse DEM were erased and then filled in using a natural neighbor interpolation between the topographic shoreline and offshore bathymetry. This introduces uncertainty into inundation modeling, because wave heights and inundation are sensitive to near-shore bathymetry especially if the bathymetry is complicated. *Shuto et al., (1986)* examined the effects of modeling runup with low resolution bathymetry and determined the condition that a wavelength-dependent resolution of 20 cells per wavelength is required to avoid numerical damping of wave amplitude. This condition is met using the coarse bathymetry and for the modeled 1971 tsunami, but only up to depths of 8m. However, the grid size in this shallow region has been resampled down to the 3 arcseconds, so numerical damping should not be an issue, although missing details in the nearshore bathymetry are still potentially a large source of error.

To test the sensitivity of wave height and runup to the presence of Kamchatsky and Pokaty canyons, the models were run with a modified bathymetry, in which the canyons were artificially "filled" in. Like the stitching process outlined above, the canyons were cut out of the bathymetry and then a natural neighbor interpolation filled in the resulting gap, approximating what the shelf would look like without the canyon.

Earthquake Sources

Inputs for the Okada Model were determined using mapped aftershock locations and from published focal mechanisms published focal mechanisms (*Cormier, 1975; Okal & Talandier, 1986*). The values for strike, dip, rake, and slip used were the same as in the *Martin et al. (2007)* study. Based on aftershock locations, the 1971 source was moved as far west as seemingly appropriate; approximately half a degree closer to Ust Kamchatsk than was previously modeld. The 1969 source was identical to the previous study (Table 2). The initial modeled sea-surface deformations are shown in Figure 12.

Model Results

1971

Modeled runup for the 1971 tsunami was highest between Kamchatsky Cape and Cape Africa (Figure 11), typically ranging from 7 to 9 meters. Runup is greatest here because of the proximity of the earthquake source and the directivity of the wave towards this southeastward facing coast. The model performed well, falling short of sediment runup at only two locations where the sediment runup was very high, north of Cape Africa. The positive wave arrives fastest at the mouth of the Perevalnaya River (Figure 13) due to the deeper water of the small submarine canyon just offshore. The pattern of modeled runup here shows that tsunami runup is very low at the mouth of the Perevalnaya River, barely exceeding the measured sediment runup. On either side of the river mouth, the runup is locally high. Unlike the measured deposit inundation, the modeled inundation is very large, suggesting that the low modeled runup is a result of low topography in the DEM. This pattern is reflected at other locations. Low points of modeled sediment runup in Figure 11 tend to correspond to peaks in inundation distance.

In Ust Kamchatsk, the modeled runup is consistently lower than the deposit runup (Figure 14), but the overall shape of the modeled runup distribution closely matches the deposit runup pattern, as well as the recent storm deposit runup pattern. Both the modeled and sediment runup peak at the east end of Dembi spit, and generally decrease towards the east. The modeled runup on the west end of the spit follows expected behavior and does not exceed 3.5 meters.

The modeled arrival of the first positive wave of the 1971 tsunami in Ust Kamchatsk is 19-20 minutes after the earthquke in Ust Kamchatsk, which closely agrees with the time (20 min) recorded on the actual tide gauge. However, the Ust Kamchatsk tide gauge record was located behind the spit and the tsunami was not modeled through the mouth of the Kamchatka river, so the modeled arrival of the wave is probably slightly late. In the filled canyon run, the wave arrives after 25 minutes, clearly illustrating that without the presence of deep water in the canyon, wave speed decreases (Figure 15). Figure 15 also displays how the tsunami refracts as it travels over Kamchatsky Canyon. Because of the faster wave speed in the deeper part of the canyon, we expect the wave refracts towards the walls, resulting in lower wave heights along the reach of the canyon (*Divyalakshmi et al., 2011*). The filled-canyon model shows some refraction due to the shape of Kamchatsky Bay, but the effects are not very pronounced. Contrary to what was expected, the wave height right on shore at Dembi Spit is 0.5 m higher in the models run with Kamchatsky Canyon filled. This is most likely due to the nature of the wave that inundates Dembi Spit. Both filled and unfilled models indicate that the wave inundating Dembi Spit is an edge wave that travels along the southern shoreline of the Kamchatsky Peninsula (Figure 16). The shallower bathymetry in the "filled" case causes greater shoaling of the edge wave, hence the greater wave height (*Gonzalez et al., 1995*). Still, the modeled runup was unchanged between models, due to the coarse horizontal resolution (30 m) of the modeled topography. As a result, the 0.5 m increase in wave height at the shoreline in the filled model did not result in inundating cells farther inland.

In Stolbovaya, the 1971 modeled runup comes close to matching sediment runup, though it is still lower at most profiles (Figure 10). After the wave refracts around the northeast corner of the peninsula, it moves fastest along Pokatiy Canyon with slight focusing of wave height toward the walls. Although sediment runup is highest (excluding profile 300) right at the head of the canyon (profile 100), the 1971 model predicts very low runup. However, the model also significantly undershoots sediment runup at profiles 1000 and 300, far away from the head of the canyon. Overall, there is no great discernible pattern in the modeled runup that is clearly explained by bathymetry. Like Ust Kamchatsk, the modeled runup did not change between models run with the original and filled bathymetry.

1969

For the 1969 tsunami model, the region south of the Ozernoi Peninsula demonstrates the best agreement between modeled and deposit runup (Figure 17). This is not surprising because, like the Cape Africa to Kamchatsky Cape region for the 1971 tsunami, this region is close to the earthquake, and its southern shorelines are parallel to the long axis of the tsunami-generating slip. Runup is lower than at Kamchatsky Cape, but this due to the smaller size and magnitude of the 1969 earthquake.

In Stolbovaya, 1969 runup is slightly lower than the modeled 1971 results, and still lower than sediment runup (Figure 10). Although Stolbovaya is located close to the southern edge of the rupture area, modeled wave heights are relatively low in southern Ozernoi Bay because most of the wave energy radiates towards the Ozernoi Peninsula or out into the Bering Sea. The wave that accounts for the inundation in Stolbovaya is a refracted part of the wave that is initially moving into the Bering Sea. As the wave travels along Pokatiy Canyon, there is some slight focusing toward the sides, though the effects are very minor and do not appear to be reflected in the inundation patterns for the model or from the observed deposits.

DISCUSSION AND CONCLUSIONS

Issues with modeled topography

Although the 1969 and 1971 models appear to account for sediment runup along the Ozernoi and outer Kamchatsky Peninsulas, the disagreement between modeled and sediment runup at Ust Kamchatsk and Stolbovaya suggest the modeled results are not entirely accurate. Besides the modeled initial conditions for the tsunami, the modeled topography is perhaps the largest source of error. The DEM used in the model exhibits topographic profiles that are consistently smoother and less steep than the actual topography in Ust Kamchatsk (Figure 18), where modeled runup is consistently lower than sediment runup . In comparison, the modeled topographic profiles are closer to reality at Kamchatsky Cape and the Perevalnaya River, where modeled runup greatly exceeds sediment runup. Figure 19 shows that localities near Cape Africa, along profiles where the DEM is less steep than measured topography, the modeled runup tends to be slightly low. The only profiles in Stolbovaya where modeled runup equaled or exceeded sediment runup had steeper slopes than what was measured (Figure 20). At the other profiles, the DEM slopes were low and modeled runup did not match sediment runup. All of these observations suggest that inundation modeling is sensitive to topographic steepness and the inaacurate representation of topography in the model is likely a large source of error.

Possible submarine-landslide source for tsunami inundation in Ust Kamchatsk

The modeled runup in Ust Kamchatsk clearly undershoots the sediment runup by at least 5 m in most cases. As a result, it seems probable that a submarine landslide offshore Dembi Spit caused generated a small tsunami with locally high runup. Based on the high runup along the eastern end of the spit and (inferred) lower runup along the western half, the landslide most likely occurred along the eastern wall of Kamchatsky Canyon. Submarine landslides often occur in canyons, especially near river deltas where large amounts of unconsolidated sediment are available so Kamchatsky Canyon is an ideal place for such an event to occur. If a submarine landslide did occur along the eastern canyon wall, I would expect to see an edge wave traveling along the southern coast of the Kamchatsky Peninsula, similar to what was predicted in the model of the 1971 tsunami. Although the actual runup values differ, the patterns of modeled, storm deposit, and tsunami deposit runup might potentially indicate a characteristic pattern unique to inundation by edge waves (Figures 6, 14).

Timing of a proposed landslide is unknown although a closer comparison of the tide gauge record in Ust Kamchatsk and the synthetic wave form from modeling the 1971 event could possibly indicate the occurrence of a submarine landslide generated tsunami *(Ma, Satake, Kamamori 1991*). One restrictive factor is that the Ust Kamchatsk tide gauge was located behind Dembi Spit and its exact location is unknown. Because the tsunami traveled through a river inlet over shallow and possibly evolving bathymetry, it is unclear whether or not comparing modeled wave heights to the actual tide gauge record is worthwhile. It is possible that the relatively short-wavelength wave from a landslide-generated tsunami would have mostly dissipated before reaching the Ust Kamchatsk tide gauge. As discussed above, the precise arrival time at the Ust Kamchatsk tide gauge of the modeled earthquake tsunami is difficult to determine because of the tide gauge location. Nevertheless, further modeling of hypothetical storm waves and land-slide tsunamis using higher resolution bathymetry and topography could help determine whether the patterns of modeled, tsunami deposit, and storm deposit runup are indicative of edge waves, and if the modeled tsunami arrival times are accurate.

Although the 1969 and 1971 models both undershoot sediment runup at Stolbovaya, there isn't as pressing a need to invoke a submarine landslide-generated tsunami. Unlike Ust Kamchatsk the models account for deposit runup at a few locations, and the discrepancy between modeled and sediment runup is typically around 1 meter, compared to at least 5 meters at Ust Kamchatsk. It is possible the 1969 and 1971 models could match sediment runup using more accurate input topography with steeper slopes, or perhaps by changing the earthquake sources.

At the mouth of the Perevalnaya River, adjacent to the small, unnamed submarine canyon, the modeled runup clearly exceeds the deposit, so the 1971 tsunami accounts for the runup here. Even though modeled offshore waveheights at the head of the canyon were lower here than in the case with canyons filled, this did not translate into significantly lower runup. This suggests that any number of factors, including near-shore bathymetry, and onshore topography and roughness influence runup more than relatively minor (<1m) changes in offshore wave height due to refraction over submarine canyons.

Conclusions

We were able to identify tsunami deposits near Ust Kamchatsk, post-dating 1964. Even though the 1971 Kamchatsky tsunami would have been the most likely source of these deposits, the modeled tsunami runup is significantly lower than sediment runup, suggesting that the maximum deposit runup cannot be explained solely by the earthquake-generated tsunami. Based on the spatial distribution of sediment and modeled runup, as well as the nearby presence of a steep-walled submarine canyon, a submarine-landslide generated tsunami is the most plausible explanation for the high sediment runup. However, uncertainty in the modeled tsunami runup due to inaccurate modeled topography and imprecise earthquake source characteristics could potentially account for some of the discrepancy between modeled and sediment runup. This is especially likely at Stolbovaya, where the runup discrepancy is small. Therefore, a submarine landslide tsunami source does not need to be invoked for Stolbovaya, until models using higher resolution and more accurate input topography are run and suggest otherwise. The next step in determining the source of the tsunami deposit in Ust Kamchatsk is to model hypothetical submarine landslide tsunamis and storm surge, ideally using higher resolution bathymetry.

In just a handful of cases, and only with access to very high-resolution bathymetry, detailed tide gauge records, or other fortuitous observations, have tsunamis been definitively linked to submarine landslide sources. In terms of data availability and quality, this study is perhaps more similar to paleotsunami reconstructions, which heavily rely on deposit data and only have very roughly determined earthquake sources. Still, the model results and deposit data presented here are able to suggest that changes in tsunami wave height due to refraction along the reach of submarine canyons are not enough to significantly reduce tsunami runup. In addition, the increased exposure to submarine landslide-generated tsunamis at the heads of large submarine canyons and the fact that the inundating tsunami can travel as an edge wave along a coastline counteract any measure of safety afforded by the wave dampening caused by refraction over the same submarine canyon.

REFERENCES

Berger, M. J., George, D. L., LeVeque, R. J., & Mandli, K. T. “The GeoClaw software for depth-averaged flows with adaptive refinement." *Advances in Water Resources* 34.9 (2011): 1195-1206.

Blott, Simon J., and Kenneth Pye. "GRADISTAT: a grain size distribution and statistics package for the analysis of unconsolidated sediments." *Earth surface processes and Landforms* 26.11 (2001): 1237-1248.

Bourgeois, Joanne, et al. "Holocene tsunamis in the southwestern Bering Sea, Russian Far East, and their tectonic implications." *Geological Society of America Bulletin* 118.3-4 (2006): 449-463.

Braitseva, Olga A., et al. "Holocene key-marker tephra layers in Kamchatka, Russia." *Quaternary research* 47.2 (1997): 125-139.

Choowong, Montri, et al. "Flow conditions of the 2004 Indian Ocean tsunami in Thailand, inferred from capping bedforms and sedimentary structures." *Terra Nova* 20.2 (2008): 141-149.

Cormier, Vernon F. "Tectonics near the junction of the Aleutian and Kuril-Kamchatka arcs and a mechanism for middle Tertiary magmatism in the Kamchatka basin." *Geological Society of America Bulletin* 86.4 (1975): 443-453.

Divyalakshmi, K. S., V. Rammohan, and MV Ramana Murthy. "Modification of Tsunami Wave by Submarine Canyon: Case Study of Multiple Canyons at South East Coast of India." *Marine Geodesy* 34.1 (2011): 2-15.

Folk, Robert L. "A review of grain-size parameters." *Sedimentology* 6.2 (1966): 73-93.

Gelfenbaum, Guy, et al. "Effects of fringing reefs on tsunami inundation: American Samoa." *Earth-Science Reviews* 107.1 (2011): 12-22.

George, D. L., and R. J. LeVeque (2006). Finite volume methods and adaptive refinement for global tsunami propagation and local inundation, Science of Tsunami Hazards 24, 319-328.

Gnibidenko, Helios S., and Liubov V. Svarichevskaya. "The submarine canyons of Kamchatka." *Marine geology* 54.3 (1984): 277-307.

Gonzalez, F., R. J. LeVeque , P. Chamberlain, B. Hirai, J. Varkovitzky, and D. L. George (2011), GeoClaw Results for the NTHMP Tsunami Benchmark Problems, [NTHMP] National Tsunami Hazard Mitigation Program. 2012. Proceedings and Results of the 2011 NTHMP Model Benchmarking Workshop. Boulder: U.S. Department of Commerce/NOAA/NTHMP; (NOAA Special Report). 436 p.

González, F. I., et al. "Edge wave and non-trapped modes of the 25 April 1992 Cape Mendocino tsunami." *Pure and Applied Geophysics* 144.3 (1995): 409-426.

Goff, J., B. G. McFadgen, and C. Chagué-Goff. "Sedimentary differences between the 2002 Easter storm and the 15th-century Okoropunga tsunami, southeastern North Island, New Zealand." *Marine Geology* 204.1 (2004): 235-250.

Jagodziński, Robert, et al. "Heavy minerals in the 2011 Tohoku-oki tsunami deposits-insights into sediment sources and hydrodynamics." *Sedimentary Geology* (2012).

Kawata, Yoshiaka, et al. "Tsunami in Papua New Guinea was as intense as first thought." *Eos, Transactions American Geophysical Union* 80.9 (1999): 101-105.

Kovalev, P. D., A. B. Rabinovich, and G. V. Shevchenko. "Investigation of long waves in the tsunami frequency band on the southwestern shelf of Kamchatka."*Natural Hazards* 4.2 (1991): 141-159.

LeVeque, Randall J. *Finite volume methods for hyperbolic problems*. Vol. 31. Cambridge university press, 2002.

Lynett, Patrick J., et al. "Field survey and numerical simulations: A review of the 1998 Papua New Guinea tsunami." *Landslide Tsunamis: Recent Findings and Research Directions* (2003): 2119-2146.

Ma, Kuo-Fong, Kenji Satake, and Hiroo Kanamori. "The origin of the tsunami excited by the 1989 Loma Prieta earthquake—Faulting or slumping." *Geophys. Res. Lett* 18.4 (1991): 637.

MacInnes, Breanyn T., et al. "Slip distribution of the 1952 Kamchatka great earthquake based on near-field tsunami deposits and historical records."*Bulletin of the Seismological Society of America* 100.4 (2010): 1695-1709.

Martin, M. Elizabeth, et al. "Combining constraints from tsunami modeling and sedimentology to untangle the 1969 Ozernoi and 1971 Kamchatskii tsunamis." *Geophysical Research Letters* 35.1 (2008): L01610.

Matsuyama, Masafumi, J. P. Walsh, and Harry Yeh. "The effect of bathymetry on tsunami characteristics at Sisano Lagoon, Papua New Guinea."*Geophysical research letters* 26.23 (1999): 3513-3516.

Minoura, K., et al. "Tsunami sedimentation associated with the 1923 Kamchatka earthquake." *Sedimentary Geology* 106.1 (1996): 145-154.

Moore, Andrew, et al. "Sedimentary deposits of the 26 December 2004 tsunami on the northwest coast of Aceh, Indonesia." *Earth, Planets, and Space* 58.2 (2006): 253-258.

Morton, Robert A., Guy Gelfenbaum, and Bruce E. Jaffe. "Physical criteria for distinguishing sandy tsunami and storm deposits using modern examples." *Sedimentary Geology* 200.3 (2007): 184-207.

Okada, Yoshimitsu. "Surface deformation due to shear and tensile faults in a half-space." *Bulletin of the seismological society of America* 75.4 (1985): 1135-1154.

Okal, Emile A., and Jacques TALANDIER. "T-wave duration, magnitudes and seismic moment of an earthquake—application to tsunami warning." *Journal of Physics of the Earth* 34.1 (1986): 19-42.

Peterson, Curt D., et al. "Paleotsunami inundation of a beach ridge plain: Cobble ridge overtopping and interridge valley flooding in Seaside, Oregon, USA." *Journal of Geological Research* 2010 (2010).

Pinegina, Tatiana K., et al. "A millennial-scale record of Holocene tsunamis on the Kronotskiy Bay coast, Kamchatka, Russia." *Quaternary Research* 59.1 (2003): 36-47.

Pinegina, T. K., and J. Bourgeois. "Historical and paleo-tsunami deposits on Kamchatka, Russia: long-term chronologies and long-distance correlations."*Natural Hazards and Earth System Science* 1.4 (2001): 177-185.

Resio, Donald T., and Joannes J. Westerink. "Modeling the physics of storm surges." *Physics Today* 61 (2008): 33.

Scoffin, T. P. "The geological effects of hurricanes on coral reefs and the interpretation of storm deposits." *Coral Reefs* 12.3 (1993): 203-221.

Switzer, Adam D., and Brian G. Jones. "Large-scale washover sedimentation in a freshwater lagoon from the southeast Australian coast: sea-level change, tsunami or exceptionally large storm?." *The Holocene* 18.5 (2008): 787-803.

Titov, V. V., and F. I. Gonzalez. *Implementation and testing of the method of splitting tsunami (MOST) model*. US Department of Commerce, National Oceanic and Atmospheric Administration, Environmental Research Laboratories, Pacific Marine Environmental Laboratory, 1997.

Zayakin, Y. A., and A. Luchinina. *Catalogue of Tsunamis on Kamchatka*. Obninsk. (1987) (in Russian).

Table 1 Summary of major historical tsunamigenic earthquakes that have registered on tide gauges in Ust Kamchtask and Hilo, Hawaii.

Earthquake	**Location**	**Moment Magnitude (M_w)**	**Max Observed Runup (m)**	**Ust-Kamchatsk Tide Gauge (m)**	**Hilo Tide Gague (m)**
15-Dec-71	Kamchatsky Bay	7.8	No data	0.45	0.15
23-Nov-69	Ozernoi Peninsula	7.7	15-Oct	0.2	0.05
24-May-60	Chile	9.5	7	0.8	10
5-Nov-52	Southern Kamchatka	9	21	0.1	1.1
14-Apr-23	Kamchatsky Bay	7.3	14-Nov	No data	0.3

Table 2 Fault parameters used to determine initial sea-surface deformation, computed using the Okada model.

Earthquake	**Fault width (m)**	**Fault length (m)**	**Slip angle**	**Dip angle**	**Strike**	**Fault disclocation (m)**	**Top center edge of fault latitude (°)**	**Top center edge of fault longitude (°)**	**Upper edge depth (m)**
1969	5000	100000	135	22	260	8	55.3	163.74	5000
1971	5000	100000	120	14	210	3.5	57.3	163.5	5000

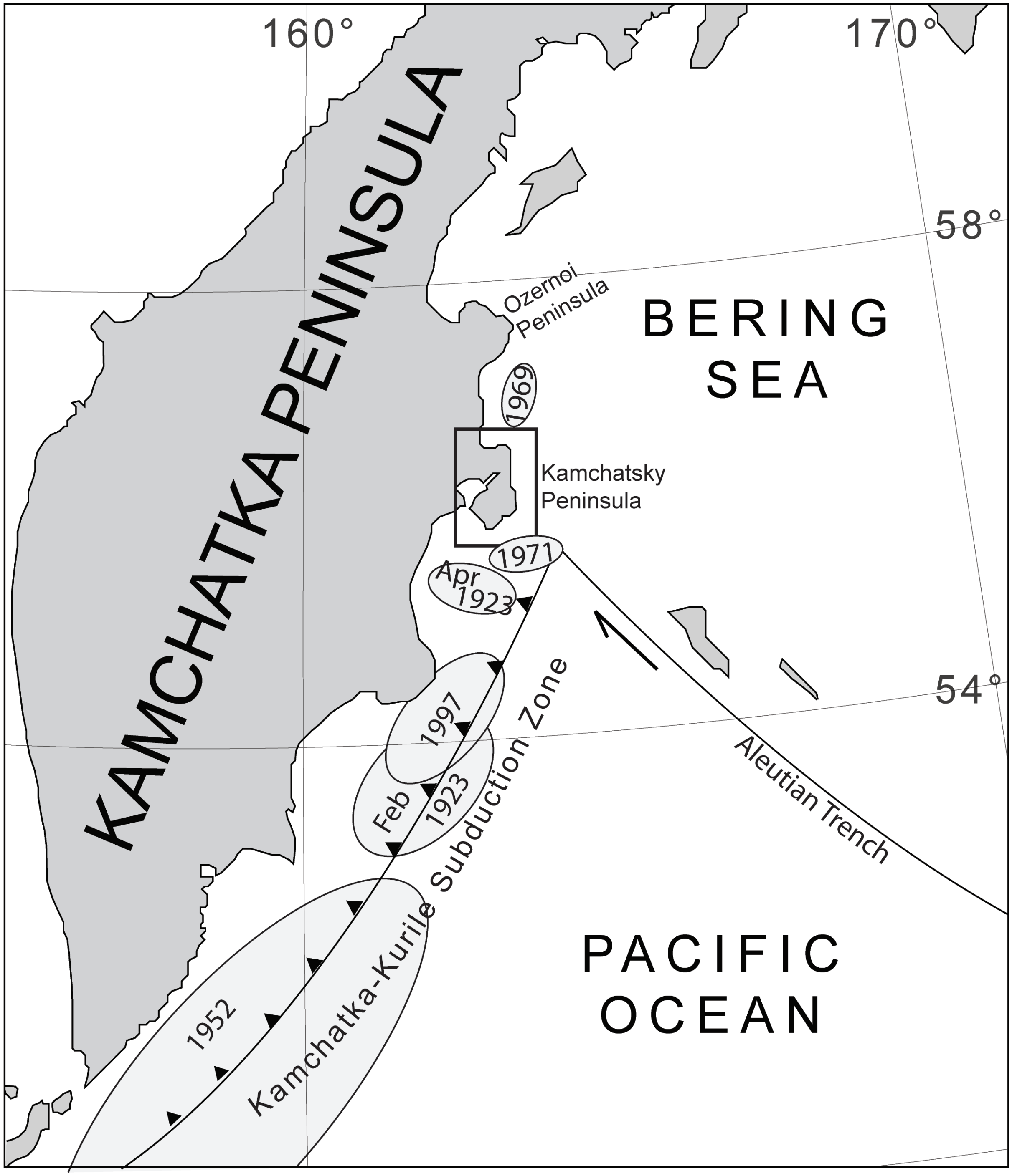

Figure 1 Location of field area (Kamchatsky Peninsula, small box), tectonic setting, and source areas of selected tsunamigenic earthquakes.

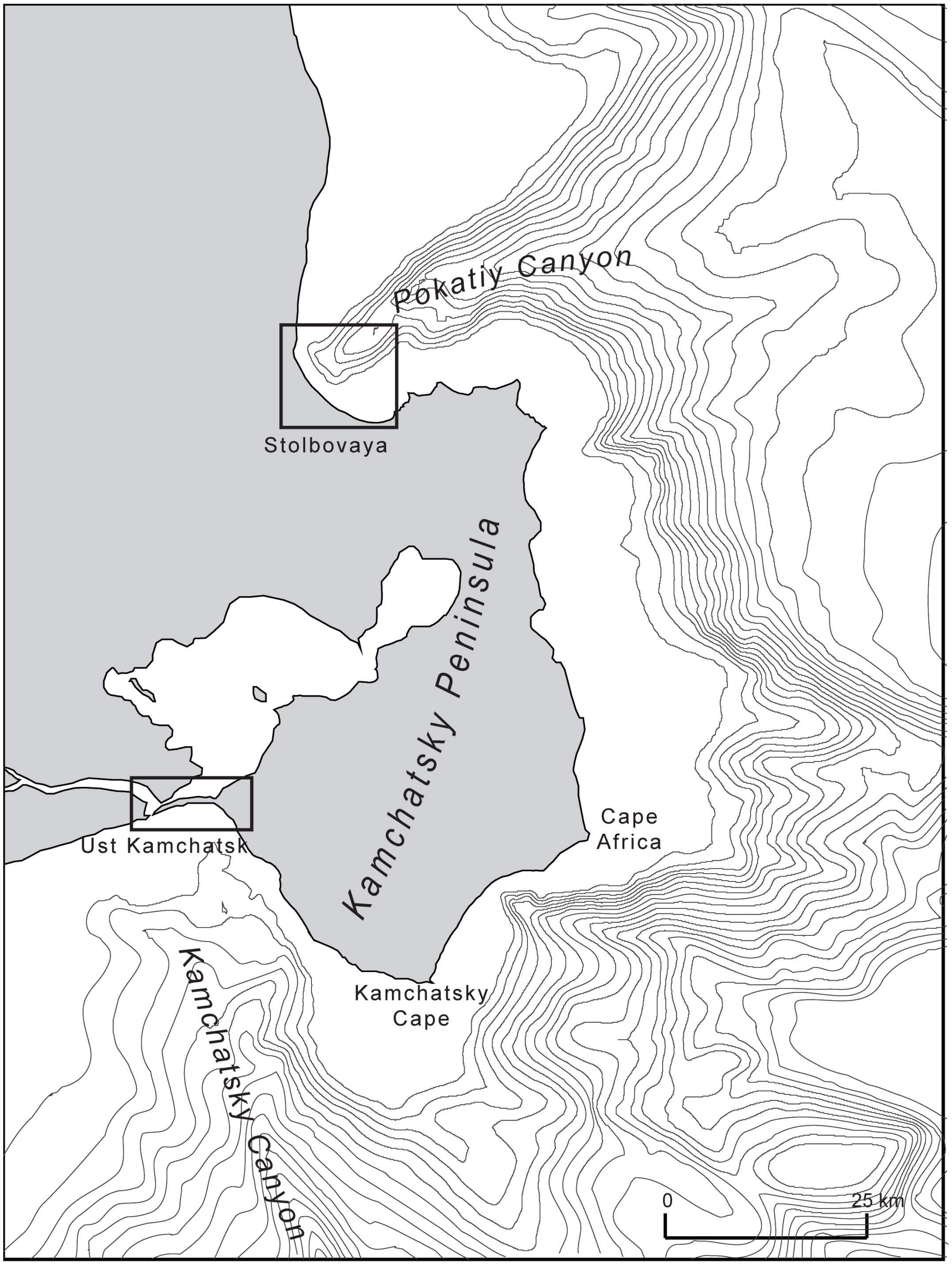

Figure 2 Map of the Kamchatsky Peninsula and offshore bathymetry. Bathymetric contour interval is 100m.

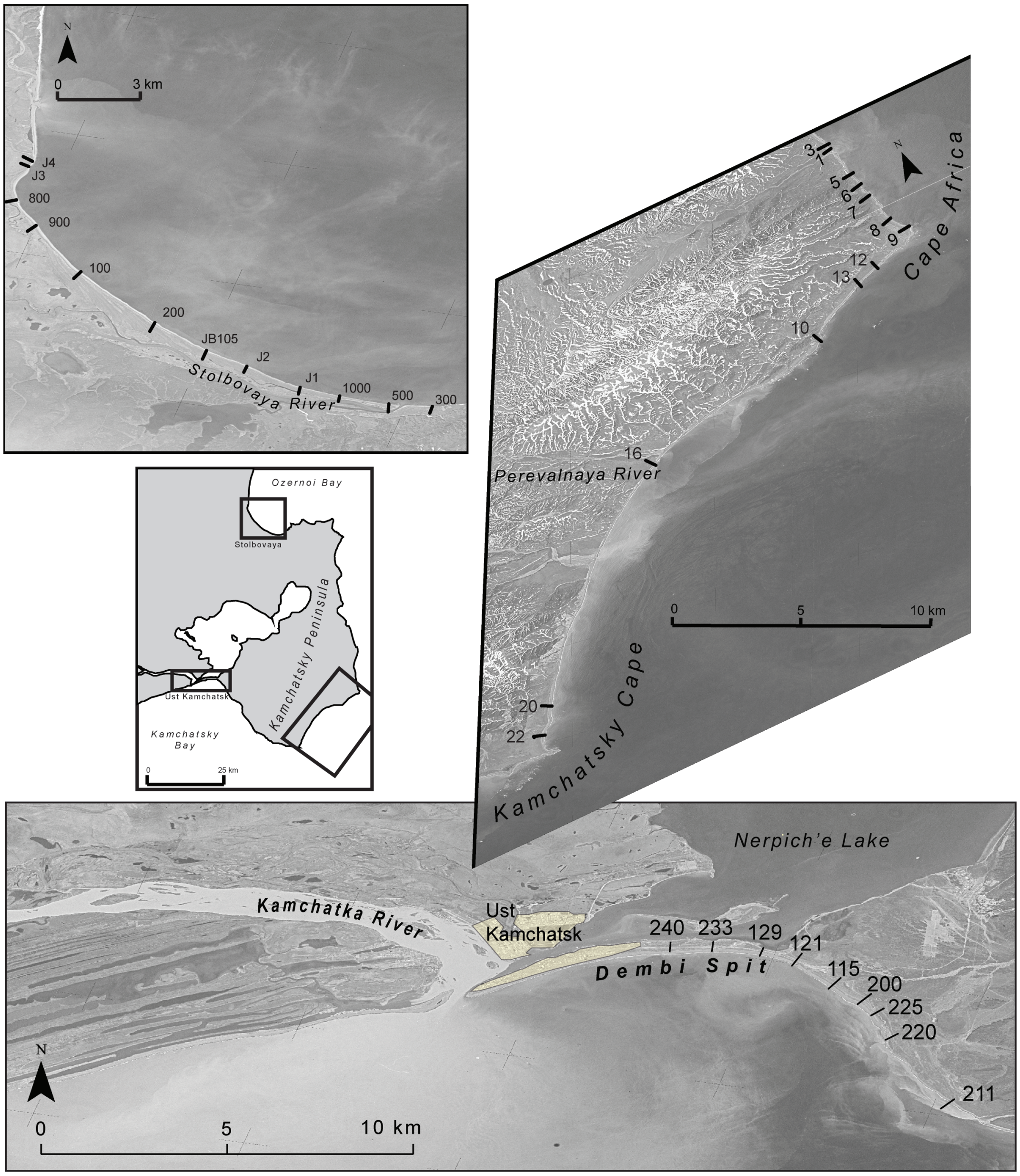

Figure 3 Aerial photos (from the 1980s) of field localities, showing locations of measured profiles. *Upper left:* Stolbovaya,

Right: Between Kamchatsky Cape and Cape Africa *Bottom:* Ust Kamchatsk (settlement highlighted in yellow).

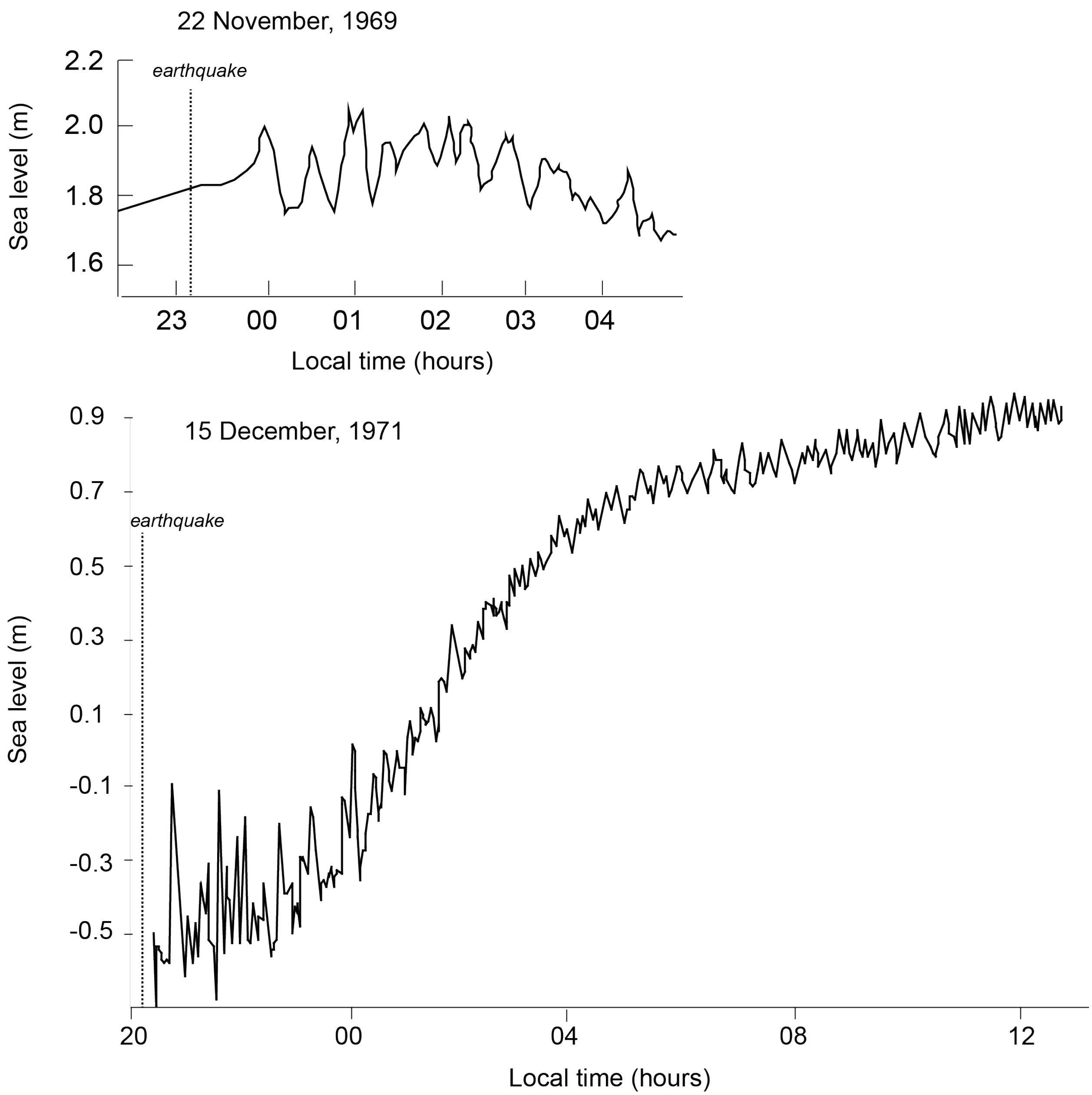

Figure 4 Tide gauge records of the 1969 (top) and 1971 (bottom) tsunamis in Ust Kamchatsk. The tide gauge was located *behind* the spit although its exact position is unknown. Timing of the earthquakes is marked by dashed lines.

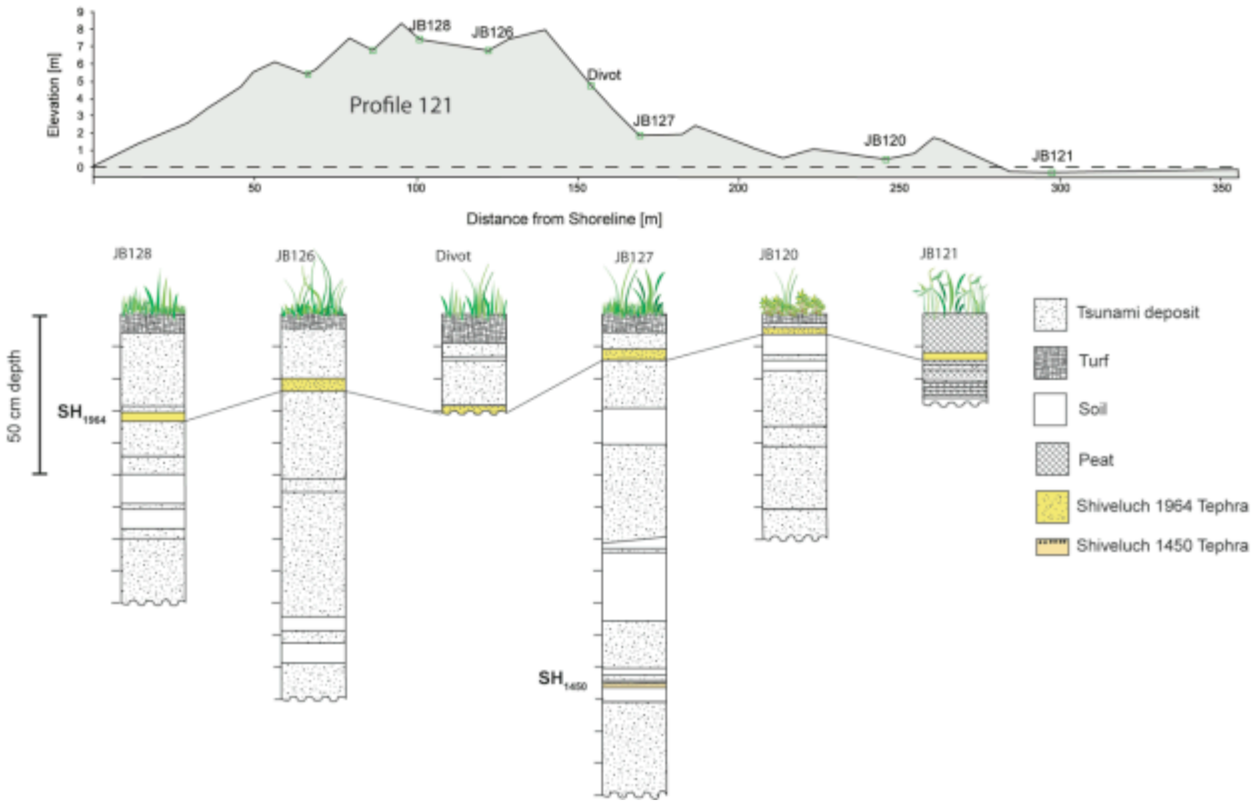

Figure 5 *a)* Topographic profile (shoreline on left) of Profile 121 on Dembi Spit, showing excavation locations. *b)* Stratigraphy of 5 excavations on Profile 121, ordered by distance from shoreline. The Shiveluch 1964 tephra is correlated between sections. Where present, the 1971 tsunami deposit lies directly on top of SH_{1964}.

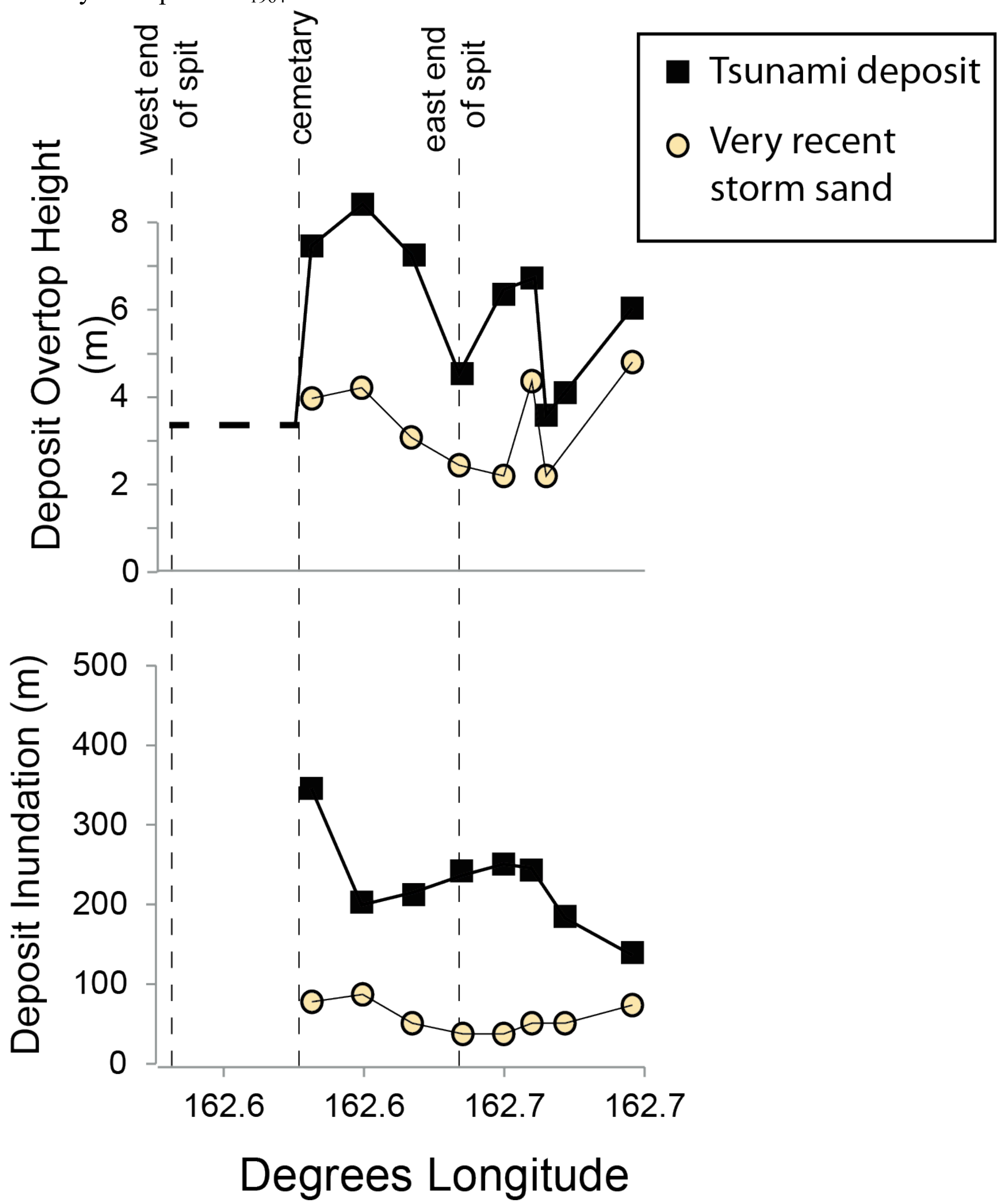

Figure 6 Comparison of runup and inundation marked by the 1971 tsunami deposit (black squares) and very recent storm sands (circles) along Dembi Spit.

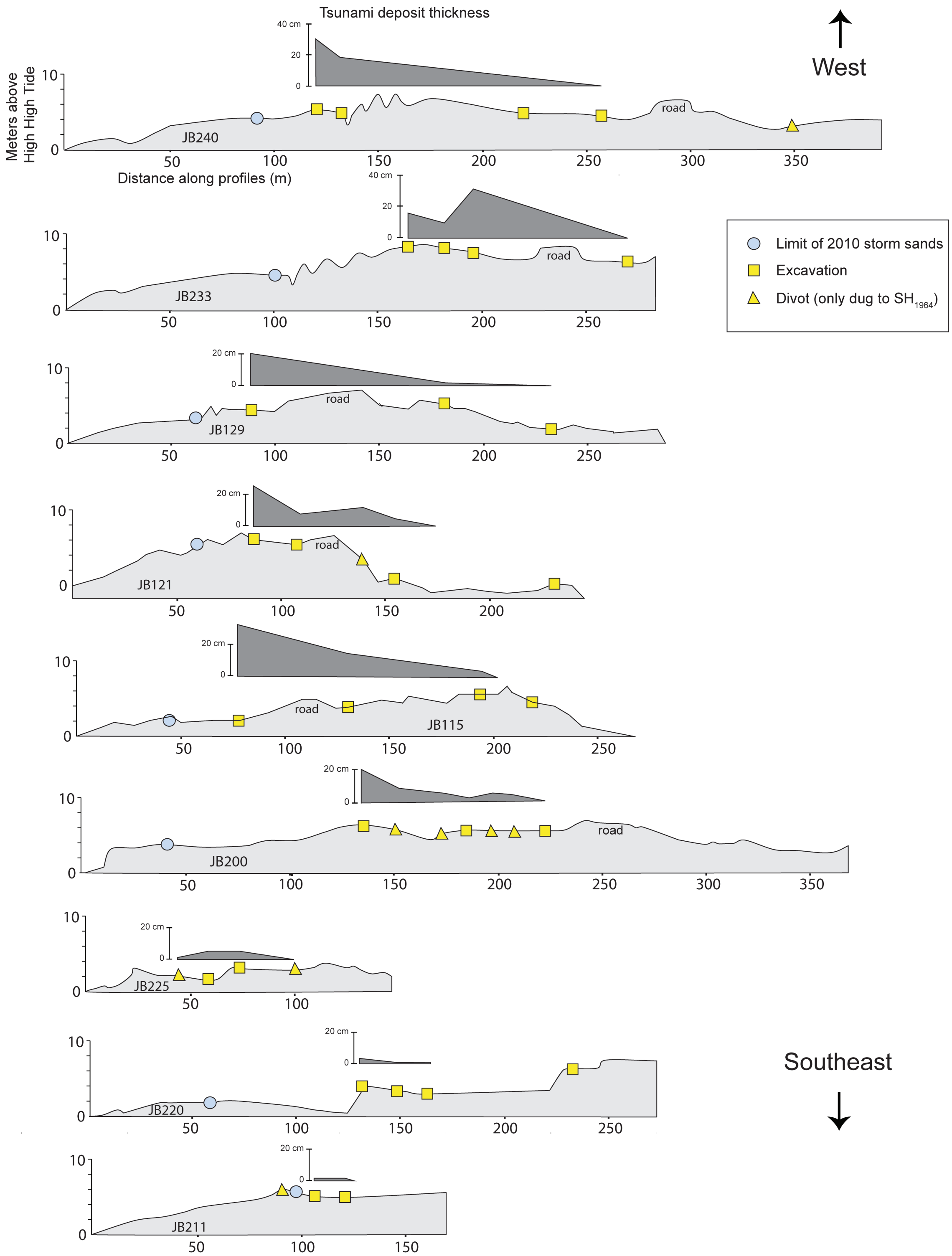

Figure 7 Ust Kamchatsk topographic profiles (light gray) and the thickness and inundation distance of the 1971 tsunami deposit (dark gray). Profile locations are shown in Figure 3. The blue circle denotes the inundation point of storm sands in 2011. Squares and triangles denote excavation and divot locations. Elevations and inundation distances are referenced to High High Tide (HHT), which is the highest swash mark found on the beach.

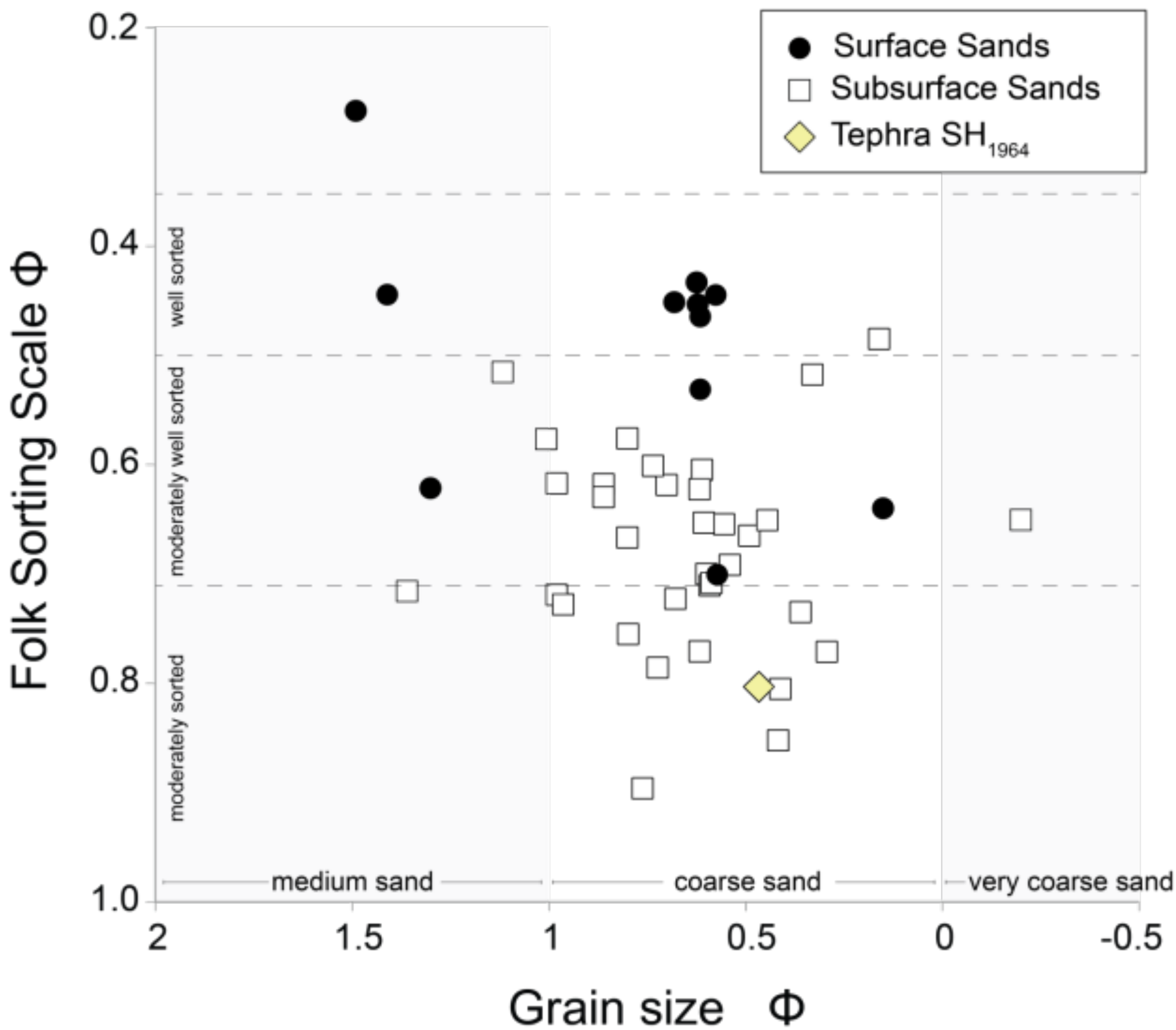

Figure 8 Grain size characteristics of sampled deposits in Ust Kamchatsk. Subsurface sands, interpreted to be tsunami deposits are represented by squares. Surface sands (modern beach and fresh storm deposits) represented by circles. One sample of the Shiveluch 1964 tephra is shown as a diamond.

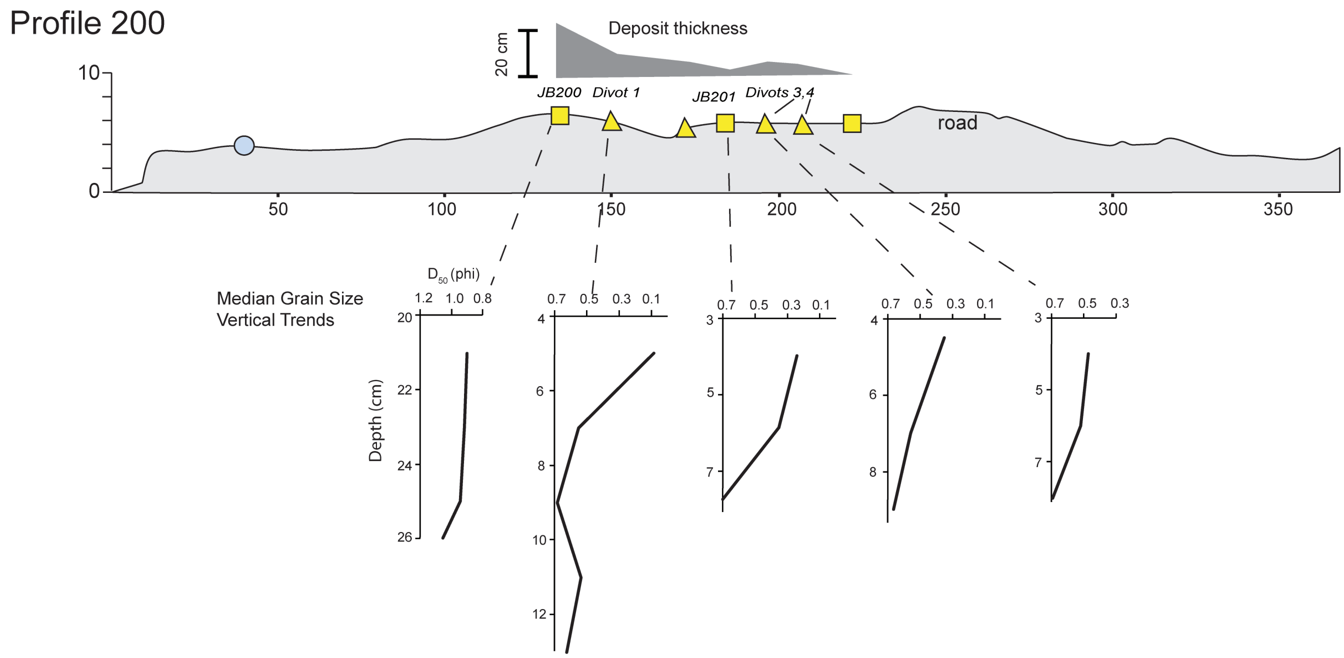

Figure 9 Vertical grain size trends of the 1971 tsunami deposit along Profile 200 in Ust Kamchatsk. Grain size is given in phi units, where medium sand ranges from 1-2 phi units and coarse sand is 0-1 phi units. Grain size trends exhibit slight upward coarsening.

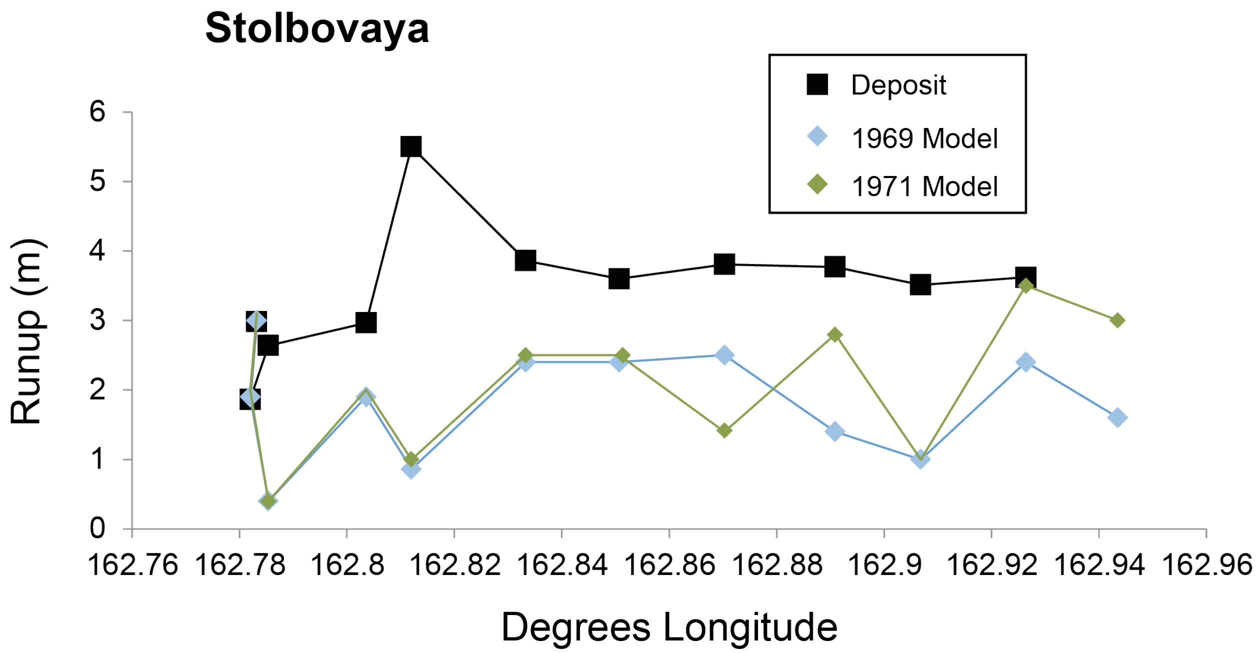

Figure 10 Runup observed (black squares) and modeled along southern Ozernoi Bay at Stolbovaya. 1969 modeled results are blue diamonds, 1971 model shown as green diamonds. Rubup for both models closely agree with each other to the west, but diverge towards the east. In most places, the deposit runup exceeds modeled runup.

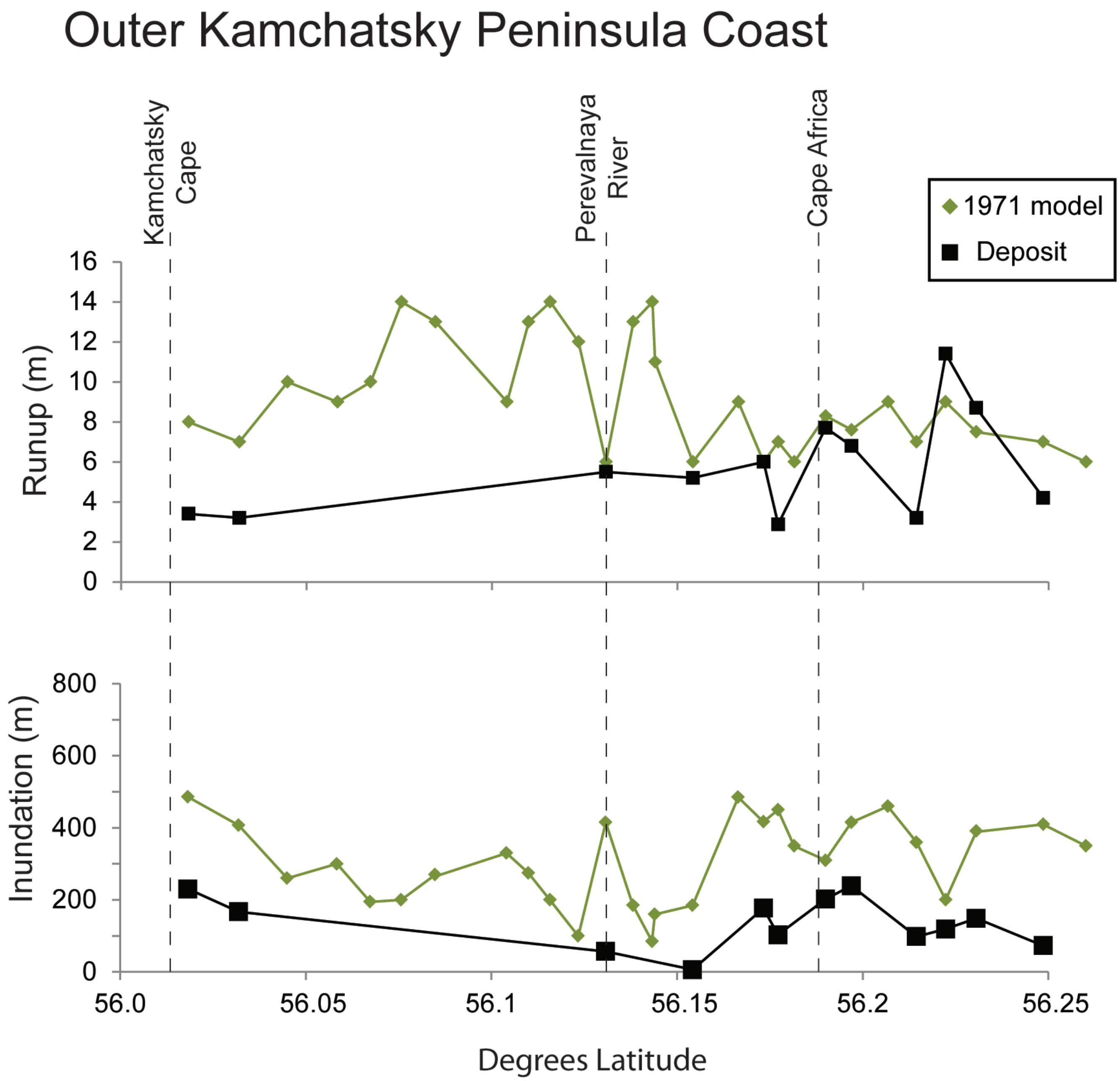

Figure 11 Modeled (green) and deposit (black) runup and inundation as a function of latitude along the outer coast of Kamchatsky Peninsula. Kamchatsky Cape, the mouth of the Perevalnaya River (at the head of a submarine canyon), and Cape Africa are indicated by dashed lines. Note that at all, but two profiles, the modeled runup accounts for sediment runup.

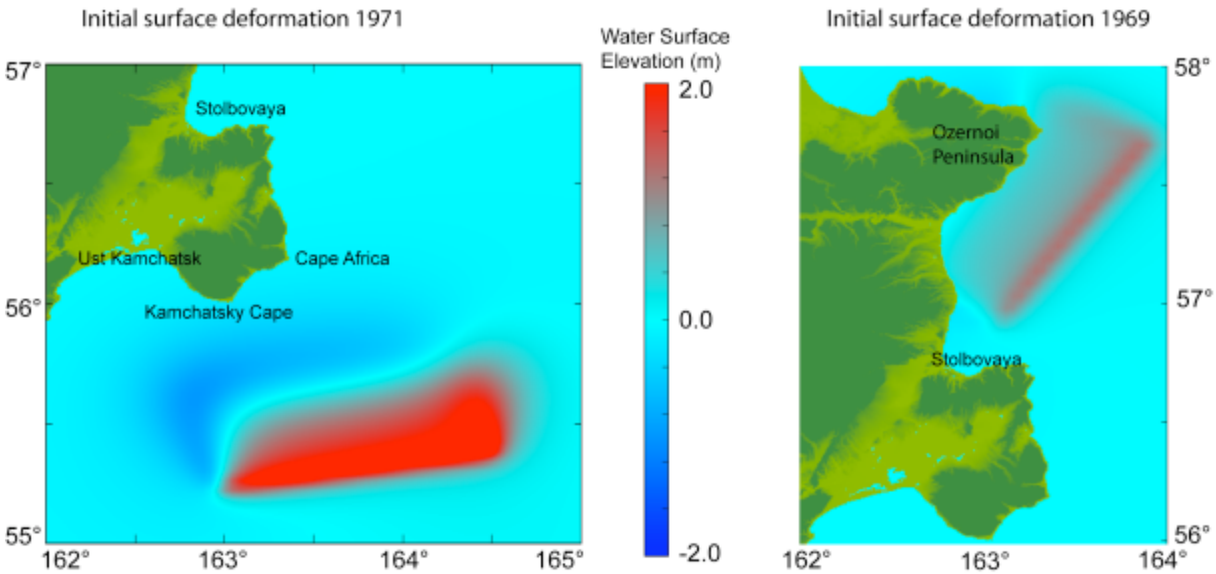

Figure 12 *a)* Modeled initial surface deformations for the 1971 tsunami. *b)* Initial surface deformation computed for the 1969 tsunami.

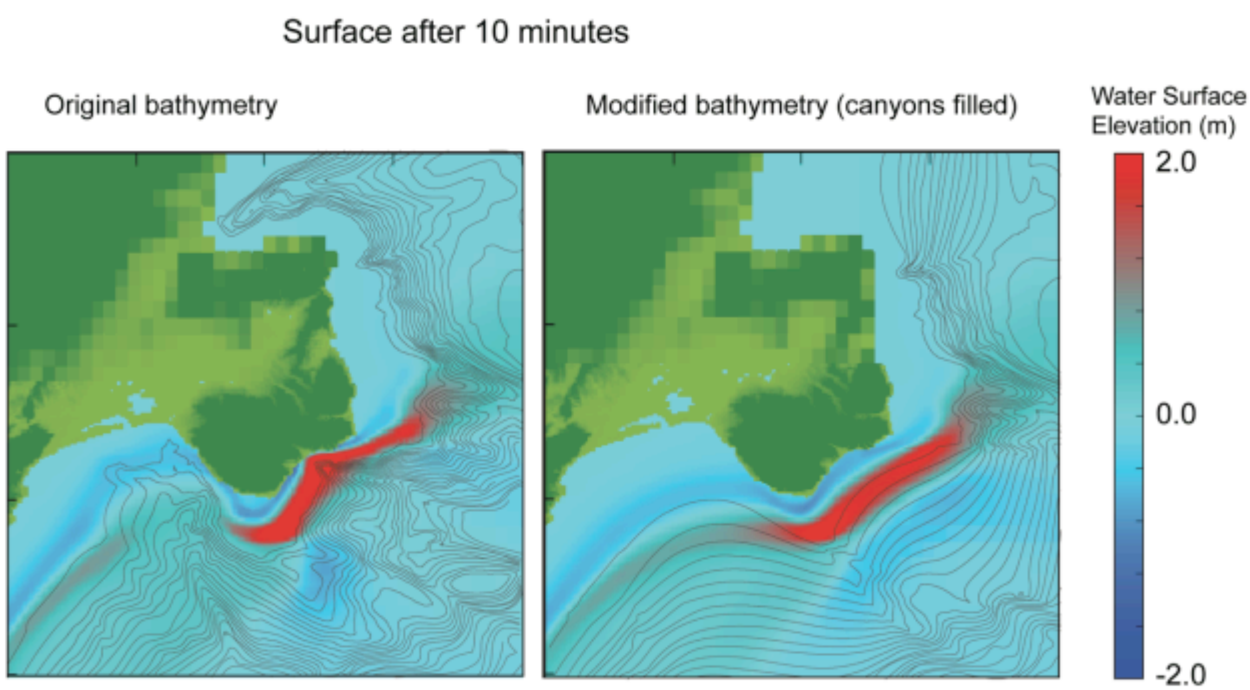

Figure 13 Tsunami wave heights 10 minutes after the earthquake. Left figure shows heights modeled using original bathymetry (contour interval is 200m). Right figure shows the model run with canyons artificially filled.

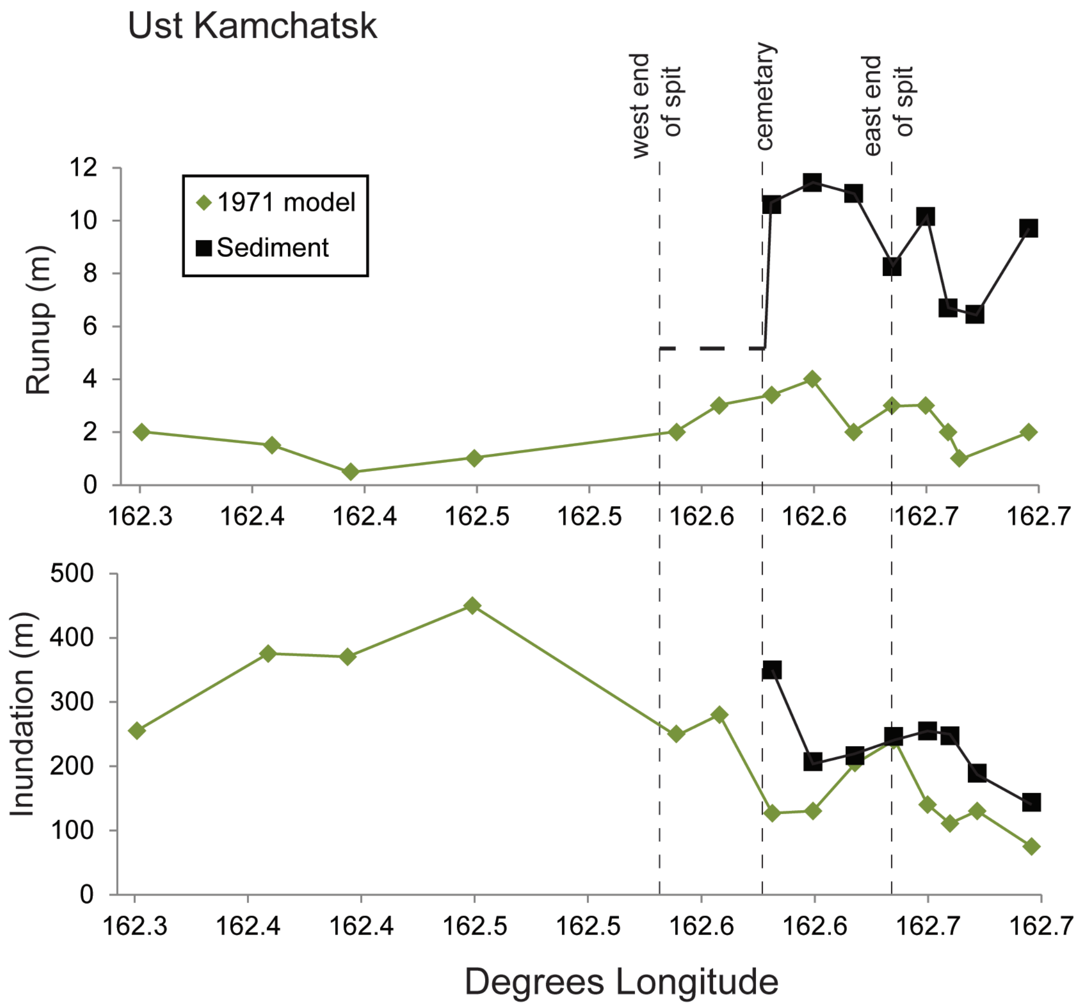

Figure 14 Runup (upper) and inundation (lower) of the 1971 tsunami in Ust Kamchatsk. Measured deposit runup and inundation is marked by black squares. The dashed line from the cemetery towards the west end of Dembi Spit represents the maximum inferred tsunami deposit, based on the elevation of buildings that were not damaged by the 1971 tsunami. Modeled runup and inundation (green diamonds) are consistently lower than for the deposit.

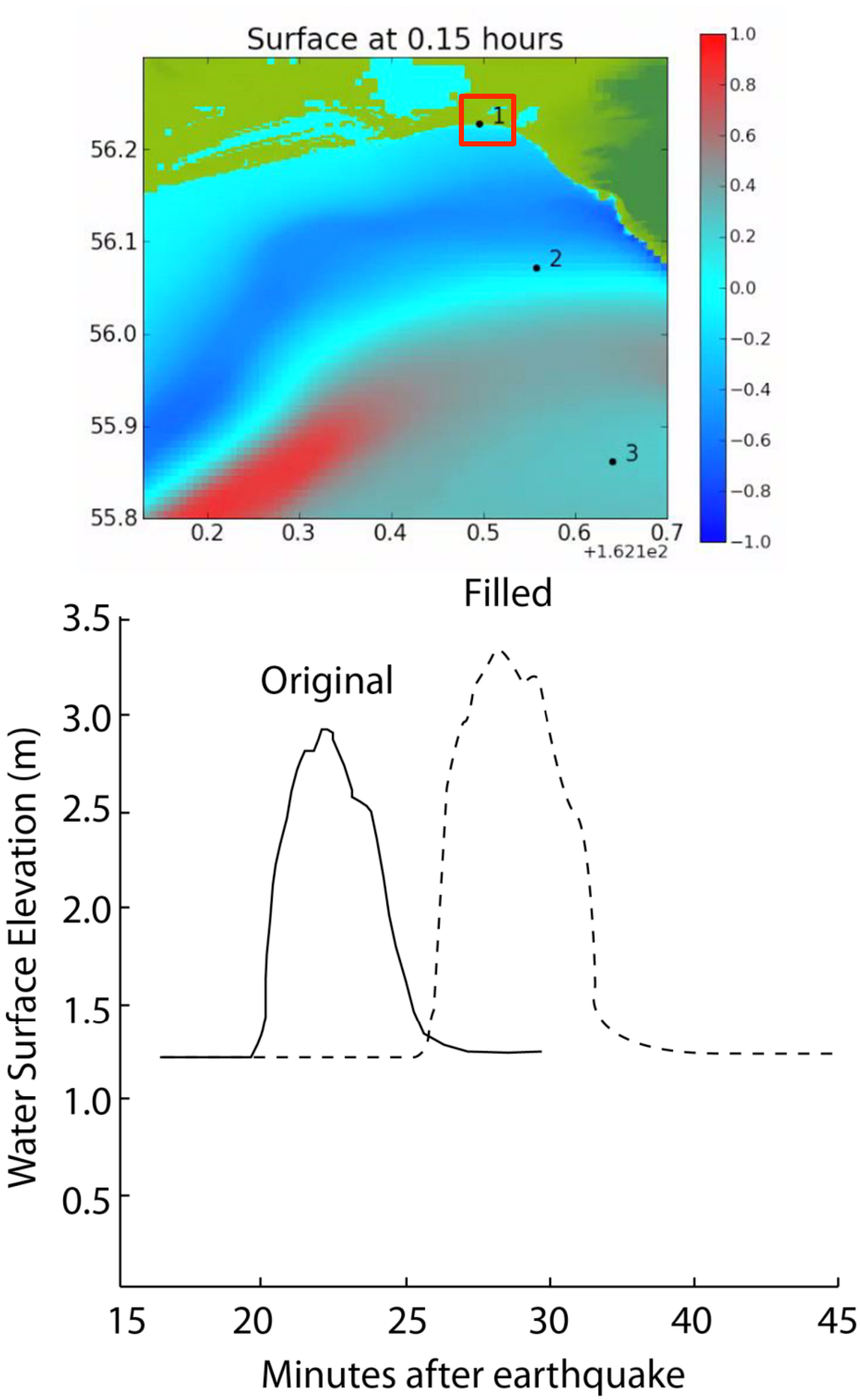

Figure 15 Onshore waveheight difference when running the 1971 model using original (with Kamchatsky canyon) and altered bathymetry (Kamchatsky canyon artificially filled). Upper map shows location of artificial tide gauge (1), corresponding to the artificial tide gauge records shown (bottom). Without the canyon, onshore wave heights are roughly 0.5 m higher.

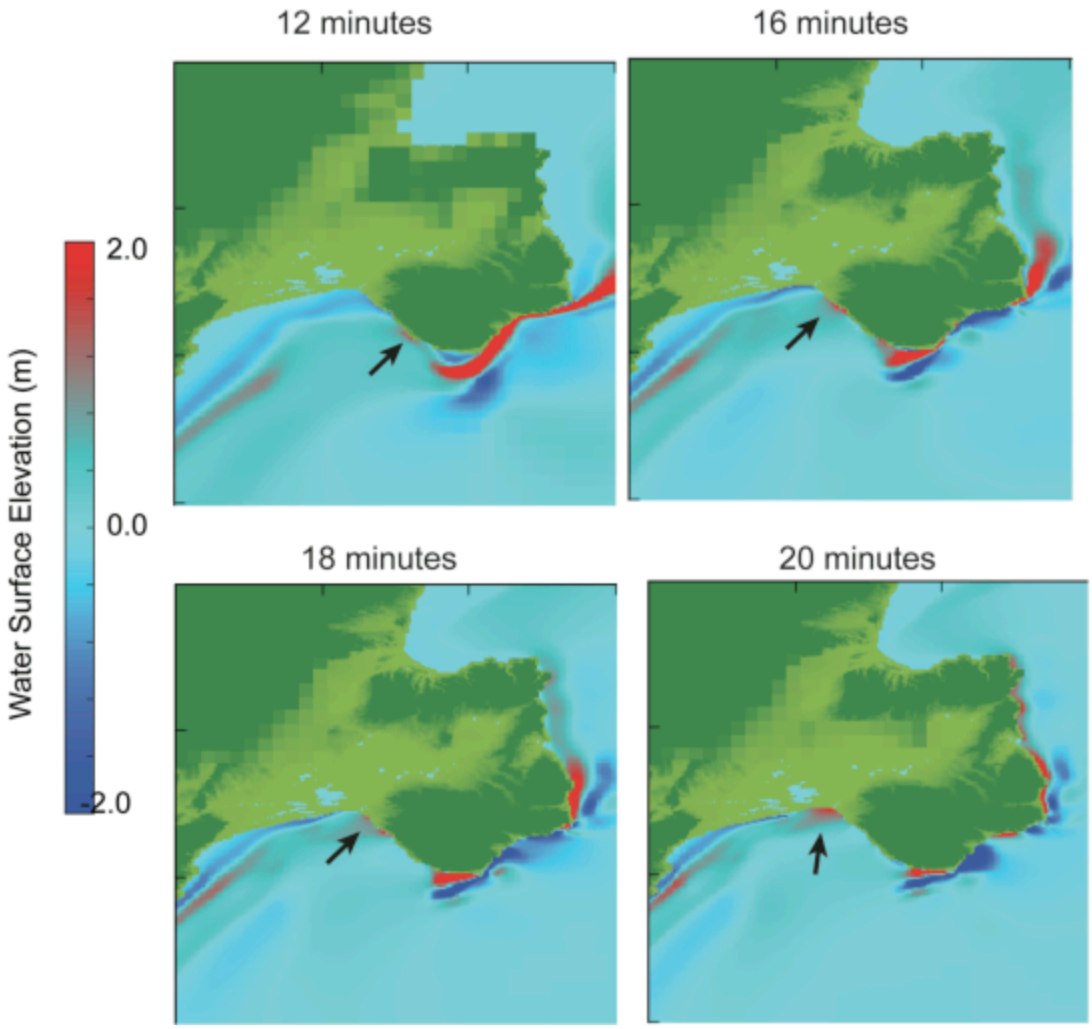

Figure 16 Modeled water surface elevation for the 1971 tsunami (using original bathymetry with canyons) at 12, 16, 18, and 20 minutes after the earthquake. The arrows are pointing out the edge wave that travels from Kamchatsky Cape towards Ust Kamchatsk

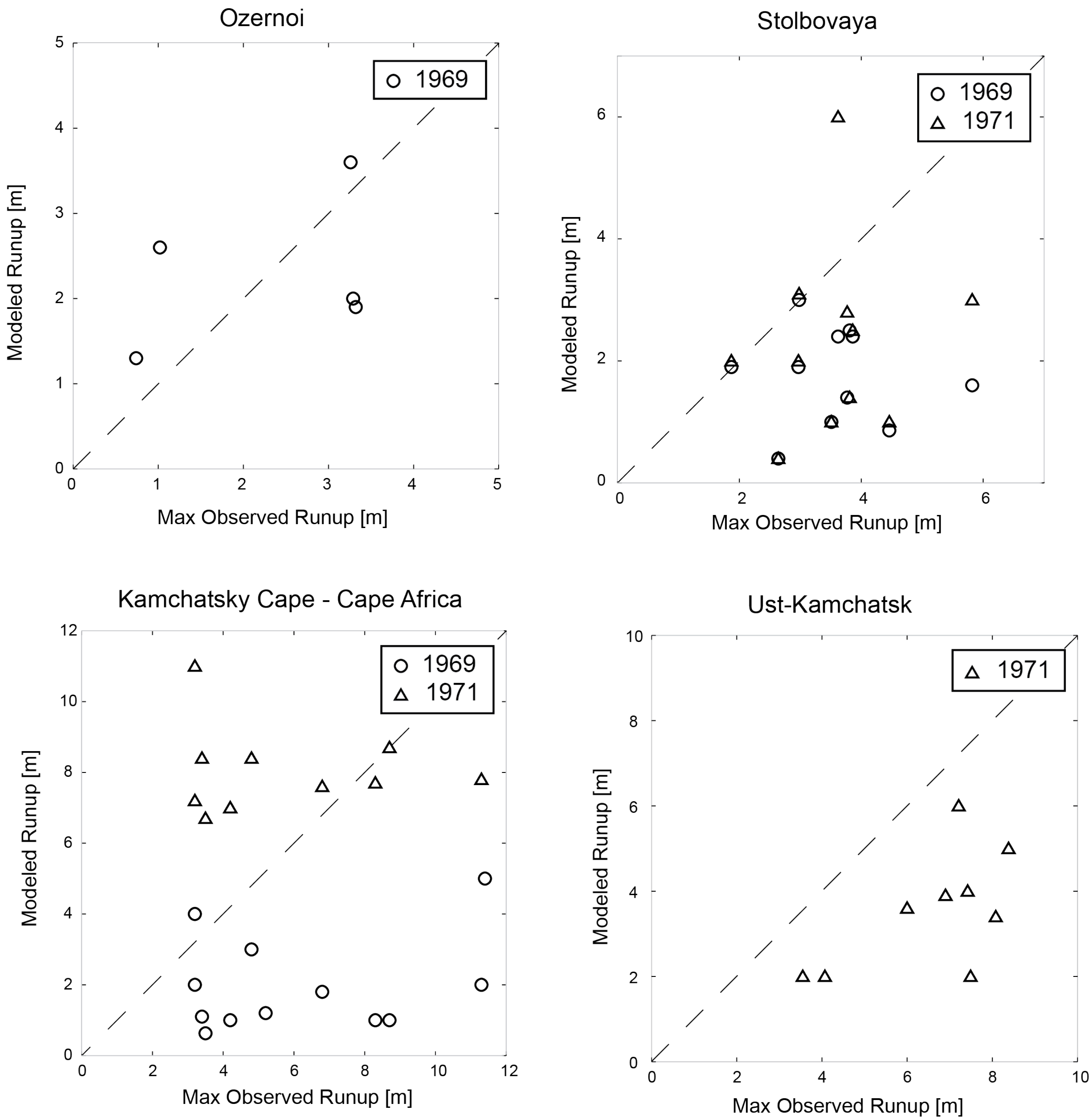

Figure 17 Modeled tsunami runup vs. observed deposit runup. The dashed line denotes perfect agreement. *a)* Results modeled for 1969 along the Ozernoi Peninsula generally exceed deposit runup. *b)* For Stolbovaya, 1969 (circles) and 1971 (triangle) model results are short of the deposit, except at a few profiles. 1971 runup tends to be slightly greater than 1969 runup. *c)* 1971 modeled results can account for deposit runup between Kamchatsky Cape and Cape Africa, while 1969 falls well short. *d)* In Ust Kamchatsk, the 1971 model is consistently short of the deposit.

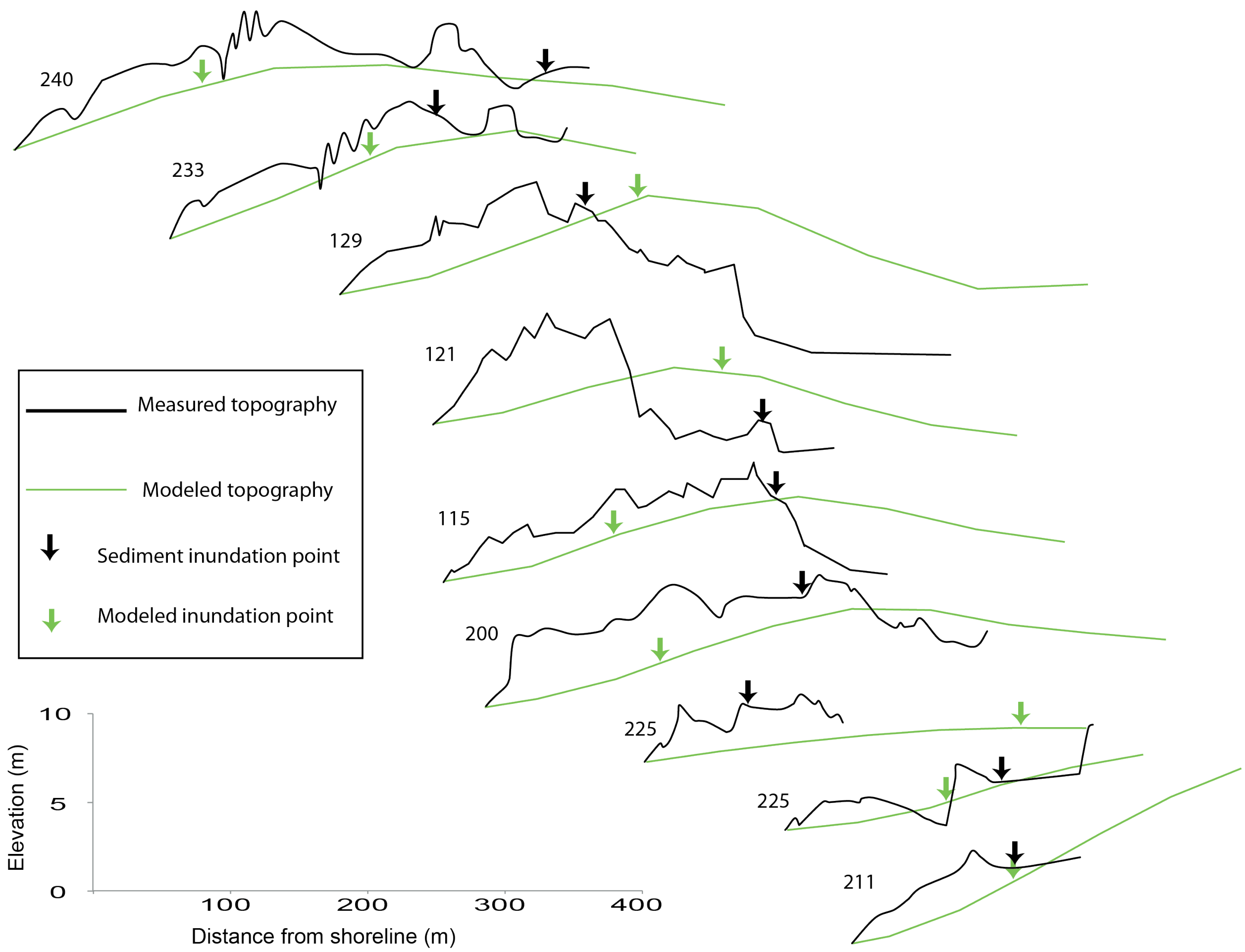

Figure 18 Comparison of topographic profiles in Ust Kamchatsk. Measured (black) and corresponding modeled (green) profiles indicate that the modeled topography is lower and shallower. Arrows denote inundation limit: black for deposit inundation, green for 1971 modeled inundation. Measured profile elevations are referenced to High High Tide (HHT). Shorelines from the DEM are determined from Mean High Water.

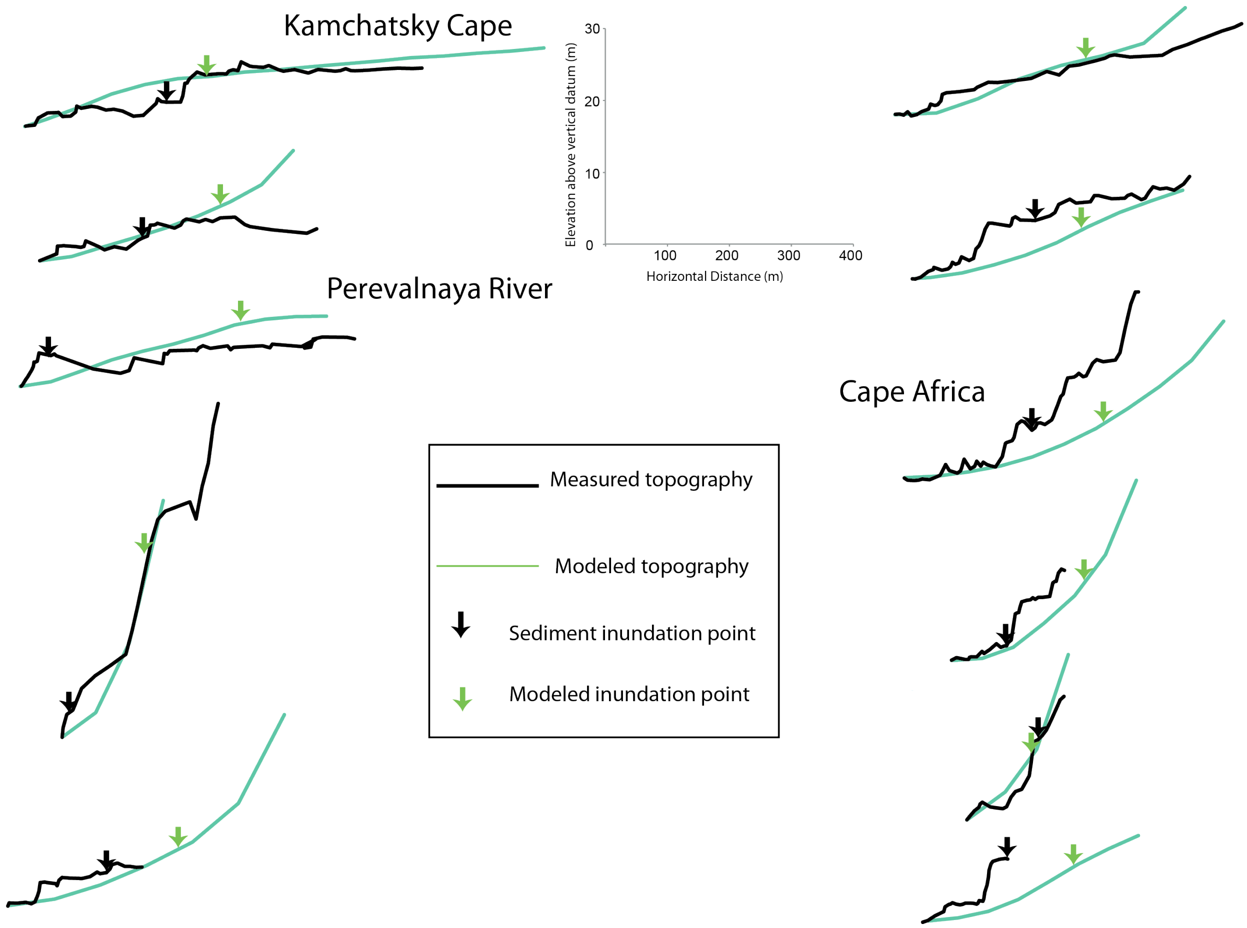

Figure 19 Comparison of measured and modeled topographic profiles between Kamchatsky Cape and Cape Africa. Black lines and arrows indicate measured topography and deposit inundation. Green indicates 1971 modeled topography and inundation. The only two profiles where sediment runup greatly exceeds modeled runup show that the modeled topography is lower and shallower than measured topography (bottom right profile and right above Cape Africa).

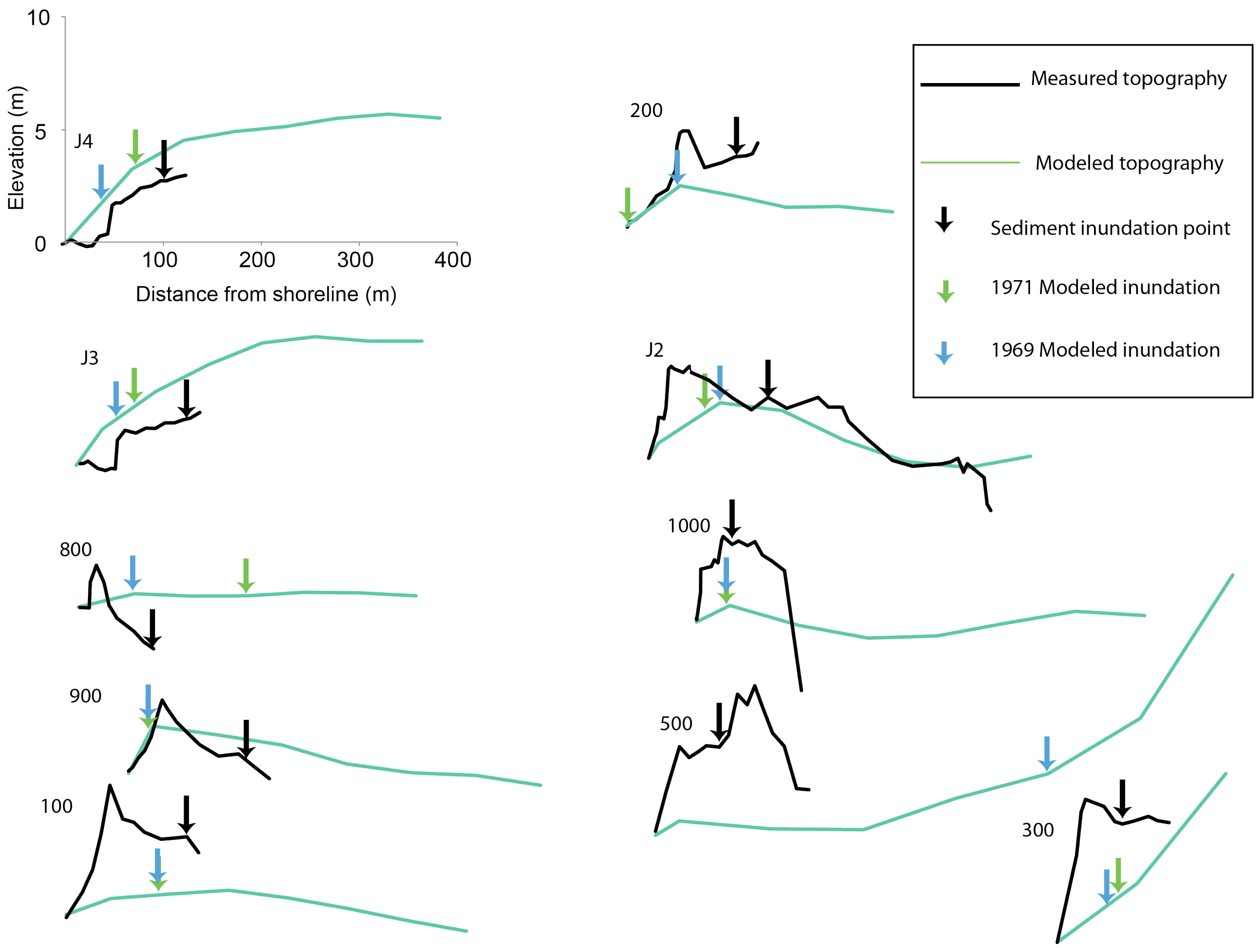

Figure 20 Comparison of measured and modeled topographic profiles at Stolbovaya. Black lines and arrows indicate measured topography and deposit inundation. Turquoise line indicates modeled topography. Blue arrow indicates modeled 1969 tsunami inundation, green indicates 1971 tsunami inundation. At profiles J4 and J3, modeled runup meets or exceeds deposit overtop heights and that in general, profiles with steeper initial slopes predict higher modeled runup.